

**PURIFICATION AND CHARACTERIZATION OF A
NOVEL ARCHAEO-EUKARYOTIC PRIMASE FROM
MIMIVIRUS**

**A THESIS SUBMITTED IN PARTIAL FULFILMENT
FOR THE DEGREE OF
MASTER OF TECHNOLOGY (INTEGRATED)
IN
BIOTECHNOLOGY**

**SUBMITTED BY
JASON C. BABY**

**UNDER THE GUIDANCE OF
DR. KIRAN KONDABAGIL**

**DEPARTMENT OF BIOSCIENCES AND BIOENGINEERING
INDIAN INSTITUTE OF TECHNOLOGY, BOMBAY**

**SCHOOL OF BIOTECHNOLOGY AND BIOINFORMATICS
D. Y. PATIL UNIVERSITY**

MAY 2015

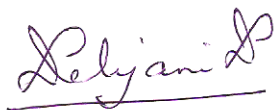
Dr. Debjani Dasgupta
Director

CERTIFICATE

This is to certify that **Mr. Jason C. Baby Susan**, M. Tech Integrated (X Semester) of the School of Biotechnology and Bioinformatics, carried out the Dissertation entitled, **“PURIFICATION AND CHARACTERIZATION OF A NOVEL ARCHEO-EUKARYOTIC PRIMASE FROM MIMIVIRUS”** for the partial fulfillment of Master of Technology (Integrated) in Biotechnology. The dissertation has not formed the basis for the award of any degree, diploma, associate-ship or fellowship. The dissertation represents independent work carried out by the candidate.

Place: Navi Mumbai

Date: 21st May 2015



Dr. Debjani Dasgupta
Director



भारतीय प्रौद्योगिकी संस्थान मुंबई
पवई, मुंबई-400 076, भारत

Indian Institute of Technology Bombay
Powai, Mumbai-400 076, India

दूरभाष/Phone : (+91-22) 2572 2545

फैक्स/Fax : (+91-22) 2572 3480

वेबसाइट/Website : www.iitb.ac.in

IIT Bombay

CERTIFICATE

I certify that the research work presented in this thesis titled “**Purification and Characterization of a Novel Archaeo-Eukaryotic Primase from Mimivirus**” has been carried out by **Mr. Jason C. Baby**, Roll No. **MTI-10007**, under my supervision and this is his bonafide work. The research work is original and has not been submitted for any degree of this or any other University. Further, he was a regular student and has worked under my guidance as a fulltime student at the Department of Bioscience and Bioengineering, IIT Bombay until the submission of the thesis to D. Y. Patil University.

Place:

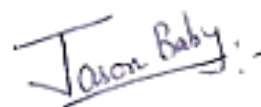
Date:

Dr. Kiran Kondabagil

Assistant Professor

DECLARATION BY THE CANDIDATE

This is to state that the work embodied in this thesis titled “ **Purification and Characterization of a Novel Archaeo-Eukaryotic Primase from Mimivirus** ” forms my own contribution to the research work carried out under the guidance of Dr. Kiran Kondabagil at the Indian Institute of Technology, Bombay. This work has not been submitted for any degree for this University or any other University. Whenever references have been made to previous work of others, it has been clearly indicated as such and included in the Bibliography.

A handwritten signature in blue ink that reads "Jason Baby:-". The signature is stylized with a long horizontal line extending from the end.

Mr. Jason C. Baby

MTI – 10007

ACKNOWLEDGEMENT

This thesis represents not only my work in the laboratory, it is a milestone of half a decade of learning and understanding at D Y Patil University, and at IIT Bombay. My experience at IIT Bombay has been nothing short of amazing. Since the first day when I joined for my project I have always felt at home here. I learnt at this place that while most people in this world only dare to wonder at the many mysteries our world presents, there are a few who have it in them, a passion, to unravel these mysteries. This thesis is a result of many such experiences I have encountered from dozens of remarkable individuals who I also wish to acknowledge. Though only my name appears on the cover of this dissertation, many individuals have contributed to its production. I owe my gratitude to all those people who have made this thesis possible and because of whom my experience here has been one I shall cherish forever.

My deepest gratitude is to my guide, Dr. Kiran Kondabagil. I have been very fortunate to have a guide who gave me the freedom to explore and understand on my own, and at the same time helped me recover and pointed me to the right direction when my steps faltered. Dr. Kiran taught me how to ask the right questions and to express my thoughts and ideas in the best way. His patience and support has helped me overcome all obstacles and finish my work. I am especially grateful to him for always going out of his way to make sure that I get the best experience possible while working with him. He remains my role model for a scientist and mentor.

I am especially indebted to my co-guide Ms. Ankita Gupta, Research Scholar at IIT Bombay. She has been the single most influential person on my development as a researcher. She has always been there to listen to me and guide me throughout the project. She taught me everything from making gels to protein purification. Her hard work and mentoring over the past six months have been instrumental in me completing my work. She is a brilliant researcher, a true friend and I know she would be an amazing professor.

Everyone in the lab provided a diverse, even if an occasionally overwhelming environment that has not only shaped me as a researcher, but also as a person.

I am grateful to Ramya for the long discussions that helped me sort out the technical details of my work. She has been my primary resource for getting my science questions answered, and an intellectual sparring partner and was instrumental in helping me crank out this thesis, and a scientific poster, all in one month. It's has been awesome to have met Amrut in the lab. He has always been a true friend, someone to sit and relax with after lab time or for advice regarding thesis writing, he is the person you can turn to for help every time. With such a different perspective from the status quo, it's always interesting to see what he thinks, especially during lab meetings. I can safely say that Avi is the rock of gibraltar of the lab, if not for her I don't think our lab could function as well as it does. She is always thoughtful in trying to make the annoying parts of lab life run more smoothly. She has been a close friend and confidante. I would like to thank Jigme for all his help and suggestions regarding troubleshooting of the issues I faced during my project. I know that I could always ask him for advice and helpful suggestions with all instrumentation and assays. I would also like to thank Supriya, she has been a constant source of encouragement and practical advice. Her advice and help in troubleshooting has helped me handle both AKTA systems and carry out protein purification successfully. Dr. Anirvan is the funniest advisor and one of the smartest people I know. He cares about and looks out for everyone in the lab. Farha has always been a great friend and it would have been a lonely lab without her. She is someone you will instantly love once you meet her.

A good support system is important to surviving and staying sane. Toward the middle and through the end of my graduate career, I had the great fortune of becoming close friends with Gokul, Anuradha and Farhan. They have helped me with the painstaking process of writing my thesis. I would also like to thank Uma for being so friendly and personable to me.

Most importantly, I would like to thank Lavanya. She was instrumental in helping me through the interview process for this internship and I will forever be grateful to her.

The influence of those with whom I worked before starting my project at IIT Bombay was also very important. Dr. Madhusudan Samant at D Y Patil University and Dr. Pravin Potdar at Jaslok Hospital provided me the foundations that allowed me to hit the ground running at IIT and complete my project successfully.

Lastly, I would like to thank my parents, Baby and Susan. My interest in science started early in my life, and they encouraged and educated me in ways both straightforward and devious. Trips to museums, books about science, chemistry experiments with stuff found in the kitchen. They have constantly supported and guided me throughout my project for which I shall be always thankful. I would also like to specially thank my elder brother, James. who has constantly guided and supported me in all aspects, without whom this thesis would not have been possible.

I also thank my friends Atharva, Dushyant, Ajinkya, Dhwani and Chintan (too many to list here but you know who you are!) for providing support and friendship that I needed to go complete this.

I express my sincere gratitude to the Head of the Department, Dr. Debjani Dasgupta, for providing me with an opportunity to conduct my thesis work in this esteemed institute.

ABSTRACT

DNA replication is a process which is common to all domains of life yet different replication mechanisms are seen among different organisms. The mechanism by which *Acanthamoeba polyphaga mimivirus* (APMV) undergoes replication is not characterized. Presence of intergenic short terminal repeats reveals that Mimivirus genome assumes a unique Q shape during replication. The mechanism of replication on such a structure is not yet understood. With this bigger picture in mind, we have initiated the characterization of a putative primase that is probably involved in the DNA replication and/or repair in Mimivirus.

Sequence alignment of gp0577 the protein encoded by gene L537 with other primases reveals that it contains the motifs common to the superfamily Archaeo-Eukaryotic Primase (AEP) and it aligns with Primpols, a novel type of primase which has RNA and DNA polymerase activities. Our initial analysis revealed that gp0577 probably exists as a dimer in its native state. We also identified the presence of conserved motifs: DxD, sxH, h- and Zn binding motif . Using DpnI mediated site directed mutagenesis we have generated active site mutants for all motifs. Templates of defined sequence were utilized to investigate the mechanism of primer synthesis by gp0577. Previous studies have suggested that the rate-limiting step of primer synthesis occurs during primer initiation during the formation of the dinucleotide. Thus we checked the effect of different concentrations of rNTPs involved in initial dinucleotide synthesis on primer synthesis. Consistent with this idea, increasing the concentration of NTPs required for dinucleotide synthesis increased the rate of primer synthesis, whereas increasing the concentration of NTPs not involved in dinucleotide synthesis inhibited primer synthesis. Further studies using radiolabelled α -³²P and γ -³²P rNTPs can be performed to estimate the length of primers formed.

TABLE OF CONTENTS

1. INTRODUCTION	1
2. LITERATURE REVIEW	3
2.1 Nucleocytoplasmic Large DNA Viruses:	3
2.2 Classification of Nucleocytoplasmic Large DNA Viruses:	7
2.3 Acanthamoeba polyphaga mimivirus:	9
2.3.1 Mimivirus Genome	11
2.3.2 Mechanism of replication in Mimivirus	12
3.1 Primases	15
3.1.1 Types of Primases	17
3.1.2 Mechanism of Primer synthesis	18
3.1.3 A novel primase-pyrophosphatase assay	19
3. MATERIALS AND METHODS	21
3.1 Purification of wild type L537	21
3.1.1 Inoculation of Starter Culture	21
3.1.2 Induction of Protein Expression	22
3.1.3 Protein Purification	22
3.1.4 Estimation of Protein Concentration	25
3.2 Introduction of H173A mutation in L537 gene	28
3.2.1 Cloning of L537 gene with H173A mutation	28

3.2.2 Transformation of L537 gene with H173A mutation in E. coli BL21 RIPL cells	30
3.3 Estimation of Primase Activity	33
3.3.1 Malachite Green Assay	33
4. RESULTS	36
4.1 Purification of wild type L537 from E. coli BL21 RIPL cells	36
4.1.1 Induction of protein expression	36
4.1.2 Affinity Chromatography – Chromatogram	37
4.1.3 Affinity Chromatography – Fractions	38
4.1.4 Size Exclusion Chromatography – Chromatogram	39
4.1.5 Size Exclusion Chromatography – Fractions	40
4.1.6 L537 wild type – Purification Profile	41
4.1.7 Estimation of the Concentration of Purified Protein	42
4.2 Introduction of H173A mutation in L537 gene from Mimivirus	48
4.2.1 Cloning of L537 gene with H173A mutation in RIPL cells	48
4.2.2 E. coli DH5 α competent cell preparation	49
4.2.3 E. coli DH5 α Plasmid Preparation	49
4.2.4 H173A sequencing result (Clone 2)	50
4.2.5 H173A induction at 30°C for 3 hours	51
4.2.6 H173A induction at 25°C for 3 hours	52
4.3 Estimation of Primase Activity	53
4.3.1 Malachite Green Assay	53

5. DISCUSSION AND CONCLUSION	56
6. FUTURE WORK	60
7. BIBLIOGRAPHY	61

LIST OF FIGURES

1. Phylogenetic tree of NCLDV's.	4
2. Features common among NCLDV's	5
3. Filtering of samples	6
4. Proposed reclassification of organisms	8
5. Transmission Electron Microscopy showing viral particles	9
6. Engulfment of virions by the host by phagocytosis.	13
7. Genome Packaging in Mimivirus	14
8. DNA polymerase extending strand synthesis from an RNA primer	15
9. tRNA priming for Reverse Transcriptase	16
10. Protein Priming mechanism	16
11. Rolling Circle replication mechanism	17
12. Mechanism of assembly of a quaternary complex	20
13. Principle of Primase- Pyrophosphatase assay	33
14. L537 induction at 30°C for 3 hours	36
15. Affinity Chromatogram for WT L537	37
16. Affinity Chromatography Fractions (Peak A)	38
17. Size Exclusion Chromatography – Chromatogram.	39
18. Size Exclusion Chromatography Fractions (II & III)	40
19. Purification profile of wild type L537	41
20. BSA Standard Curve	42
21. Protein concentration by Imaging	45
22. BSA Standard Curve (ImageJ)	46
23. DpnI digested PCR product	48

24. E.coli competent cells successfully transformed with pET28a	49
25. Plasmid purified from 12 clones of H173A DH5 α cells	49
26. 3 hour induction at 30°C	51
27. H173A induction gel	52
28. Mechanism of DpnI mediated mutagenesis	58
29. Calibration curve (Superdex 200 pg)	67

LIST OF TABLES

1. NCLDV species, hosts and genome sizes	7
2. Comparison of the genomes of different NCLDV's	8
3. NCLDV core genes found in Mimivirus	10
4. Mimivirus genes with their putative functions	11
5. Antibiotic Stock and Working Concentrations	21
6. IPTG Stock and Working Concentration	22
7. BSA Dilutions.	25
8. L537 Dilutions	26
9. Dilutions of BSA for ImageJ protein quantification	27
10. L537 Dilutions for ImageJ protein quantification	27
11. Phosphate standard curve (Dilutions)	34
12. Primase assay mix	35
13. BSA standard curve	42
14. L537 Dilutions for Bradford Assay	43
15. BSA Standard Pixel Density (ImageJ)	46
16. Phosphate Standard curve	53
17. Templates used for priming site identification	59
18. Preparation of SDS PAGE gel	65
19. Preparation of 4X Loading Dye	65
20. Preparation of 1 Litre staining solution	65
21. Preparation of 1 Litre destaining solution	66
22. Elution volume (V_e), $\log(MW)$ and K_{av} for standard markers.	66

23. Composition of Affinity Chromatography buffers	67
24. Composition of Gel filtration chromatography buffers	67
25. Plasmid purification buffers (Miniprep)	67

ABBREVIATIONS

μ	:	Micron
μL	:	Micro-Litre
μM	:	Micro Moles
bps	:	Base pairs
g/L	:	Gram/Litre
Kbps	:	Kilo Base pairs
min	:	Minute
ml	:	Milli Litre
mM	:	Milli Moles
nm	:	Nano Meter
PCR	:	Polymerase Chain Reaction
rATP	:	Adenosine Triphosphate
rCTP	:	Cytosine Triphosphate
rGTP	:	Guanosine Triphosphate
RNA	:	Ribonucleic acid
rpm	:	Revolutions per minute
rUTP	:	Uridine Triphosphate
ssDNA	:	Single stranded Deoxyribonucleic acid
tRNA	:	Transfer Ribonucleic acid
UV	:	Ultra-Violet

CHAPTER 1

INTRODUCTION

No one knows the diversity in the world, not even to the nearest order of magnitude. ... We don't know for sure how many species there are, where they can be found or how fast they're disappearing...

— *Edward O. Wilson (The Diversity of Life, 1992)*

Are viruses alive? This is a question which has confounded biologists since a long time. Several hypothesis have been proposed to explain this and the general consensus has been that viruses do not belong in the tree of life . Recently, a new viruses was identified known as *Acanthamoeba polyphaga mimivirus*, this virus falls in the family Mimiviridae (Raoult et al. 2004) under the superfamily of Nucleocytoplasmic large DNA viruses (Iyer et al. 2001). This virus has a unique repertoire of genes encoding proteins involved in replication, transcription and translation, proteins that are considered to be the hallmarks of living organisms. This discovery has blurred the once clearly defined line separating cellular organisms from viruses (Monti et al. 2006).

The origin of viral genomes was suggested to have occurred from the genomes of the cellular organisms they infect. Thus, Viruses should in fact have many genes which are cellular homologs. But on the contrary, several of the NCLDV genes have no known homologs in cellular organisms and are classified as ORFans (Forterre 2010). Studies also suggest that the ancestor of Mimivirus and other NCLDVs might have existed before the advent of eukaryotes (Koonin 2005).

In addition, mimivirus has a unique “Q” shaped topology of replicative genome (Claverie & Abergel 2009). How the genome is replicated on such a structure is not understood at all. In addition, what are the components required to operate on such a complex structure, how the replisome is formed, where and how the replication is initiated? All need to be understood. With this bigger picture in mind, in this study, we have initiated characterization of a putative primase that is probably involved in the DNA replication and/or repair in Mimivirus.

In the further chapters, the discovery and importance of NCLDV's are explained briefly, followed by a brief summary of the discovery of *Acanthamoeba polyphaga mimivirus* and its unique features, then the different types of primases and their priming mechanism are explained in brief. The next section summarizes the Materials and Methods that were followed in the course of this study, followed by the Result, Discussion, Conclusion and the Future Study.

CHAPTER 2

LITERATURE REVIEW

2.1 Nucleocytoplasmic Large DNA Viruses:

Nucleocytoplasmic Large DNA Viruses (NCLDV) form a diverse group of viruses which infect a wide array of hosts, including Eukaryotes and Protozoa. The NCLDV group was first described by Iyer et al. in 2001. They are called so because these viruses either carry out the replication of their large dsDNA completely in the cytoplasm or start their replication in the nucleus and complete it in the cytoplasm (Iyer et al. 2005). They replicate relatively independent of the host, this autonomy is possible due to the presence of 30- 50 core genes which are conserved among all NCLDV families. The proteins encoded by these genes include DNA polymerases, RNA polymerases, RNA primers, tRNA encoding genes, transcription factors, topoisomerases, helicases, ATPases. These viral genes demarcate NCLDVs as a separate class of viruses (Yutin & Koonin 2012) (Forterre et al. 2014) (Iyer et al. 2006). The discovery of *Acanthamoeba polyphaga mimivirus* has exponentially increased research in the field of NCLDVs. APMV and other members of the NCLDV family have intrigued researchers all over the world in the last decade, owing to the genome complexity and the arsenal of protein coding genes contained within them.

It has also been proposed that this group be included in a new order known as Megavirales (Colson et al. 2012). NCLDVs have been proposed to constitute a fourth domain of life besides Eukaryotes, Prokaryotes and Archaea based on various phylogenetic analysis and the presence of proteins non homologous to previously characterized proteins (Colson et al. 2012). However, this classification has been the subject of serious debate as regards to its correctness. It was also proposed that, ancient organisms belonging to a fourth domain of life may have been hosts of NCLDVs and they acquired this set of unique genes from these organisms (Yutin et al. 2014) (Colson et al. 2011) (Forterre et al. 2014).

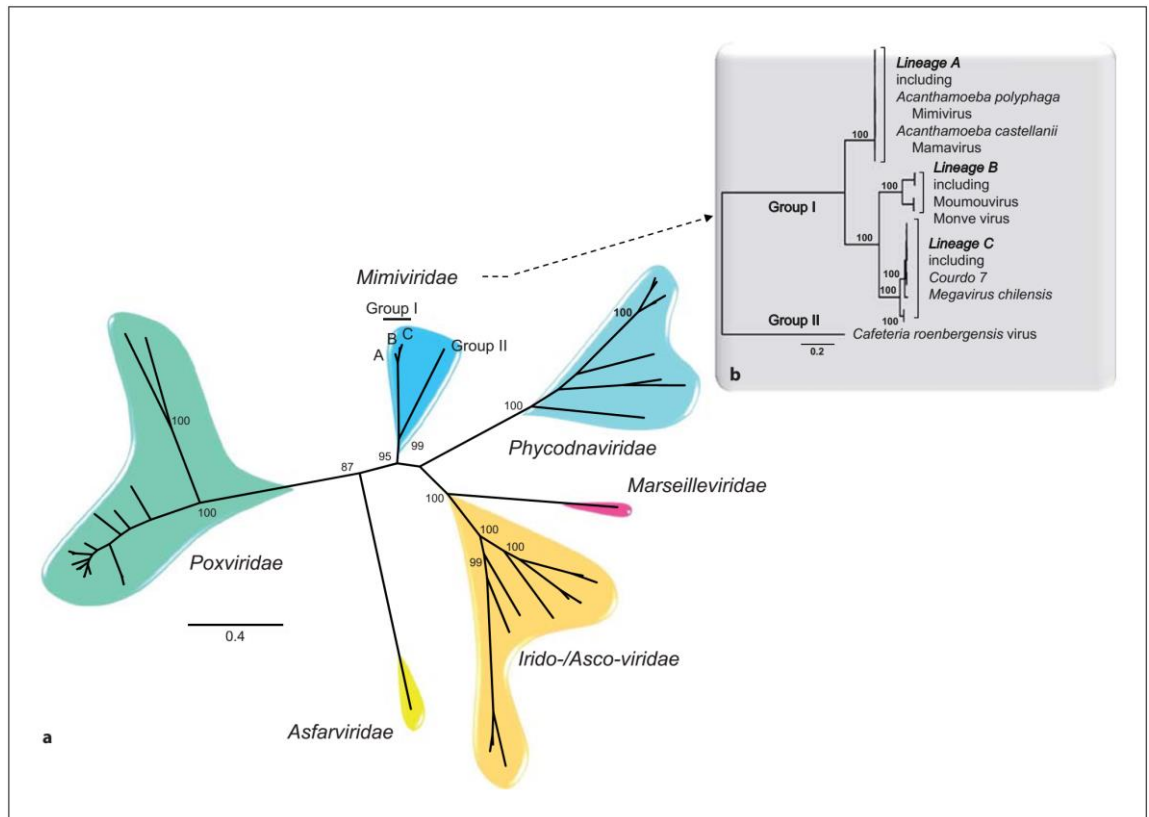


Figure 1 Phylogenetic tree of NCLDV. The tree was constructed from an alignment of 4 NCVOGs (clusters of orthologous NCLDV genes) – primase helicase, DNA polymerase, packaging ATPase and A2L like transcription factor (Colson et al. 2012).

Dissimilarity among different families of viruses?

The similarity between NCLDVs can be due to origin from a common ancestor. Generally in viral genomes, similarity is rarely seen because, even homologous viral proteins from different families show only weak sequence alignment. Such a divergence may be seen due to the rapid evolution of viral genes, but this creates a pseudo polyphyletic origin of different viral families. (Iyer et al. 2001).

Another intriguing characteristic of NCLDVs apart from their giant size is the presence of a large genome (larger than 300 kb). These large genomes encode upto 900 genes, and many of the genes common among NCLDVs are involved in DNA replication, repair, metabolism and also protein synthesis. Thus, viruses can no longer be categorized as biological entities which have a small size, small genome and extremely limited genetic information (Yamada 2011). On the construction of phylogenetic trees,

all the viral genes are generally clustered together away from cellular genes, with a few exceptions. (Filée 2013).

NCLDV's share the following common features:

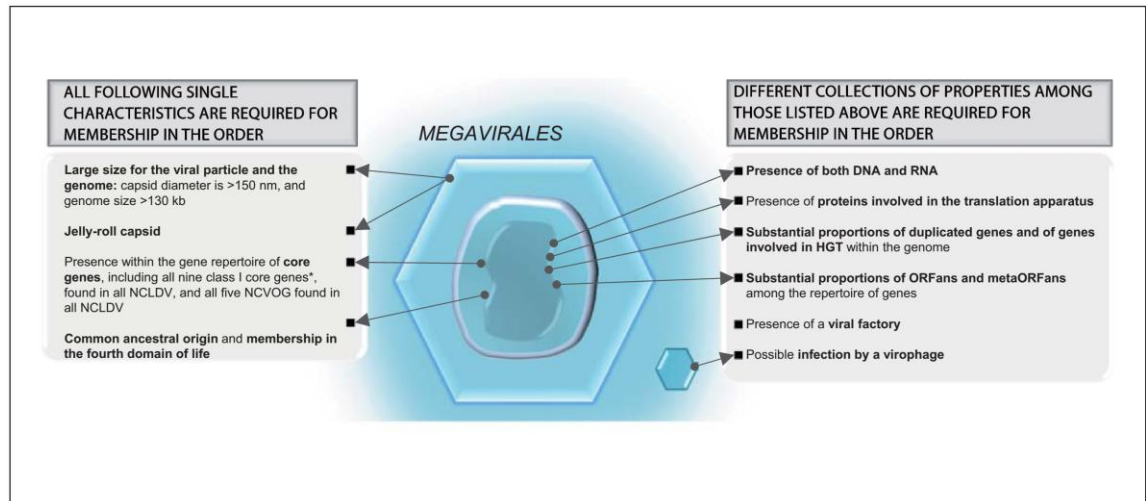


Figure 2. Features common among NCLDV's (Colson et al., 2012)

According to the current knowledge regarding the biodiversity of natural environments giant viruses are considered to be rare in the natural environment and thus it remained undiscovered for so long. But, it has eluded discovery for so long partly because of the dogma that 'members of the viral family have a small size' and the current protocols that are followed while screening for viruses have been based on this premise. Metagenomic studies involving the screening of sea water, sewage and human serum samples using modified amoebal culture methods have revealed that NCLDV's are common inhabitants of the natural ecosystems (Campos et al. 2014) (Claverie et al. 2009).

Since viruses have been classified as generally having small sizes, the practice of filtering samples prior to screening viruses is widely followed. NCLDV's have a capsid diameter ranging 0.12 μm to 1.5 μm (Colson et al. 2012) (Legendre et al. 2014), thus they have eluded detection until recent times. Also most studies regarding viruses has been focused on pathogenic viruses which infect human hosts, or on viruses which have important applications in biotechnology. However, viruses which infect protists

have not been the subject of major research, thus contributing to the elusion in their detection (Yamada 2011).

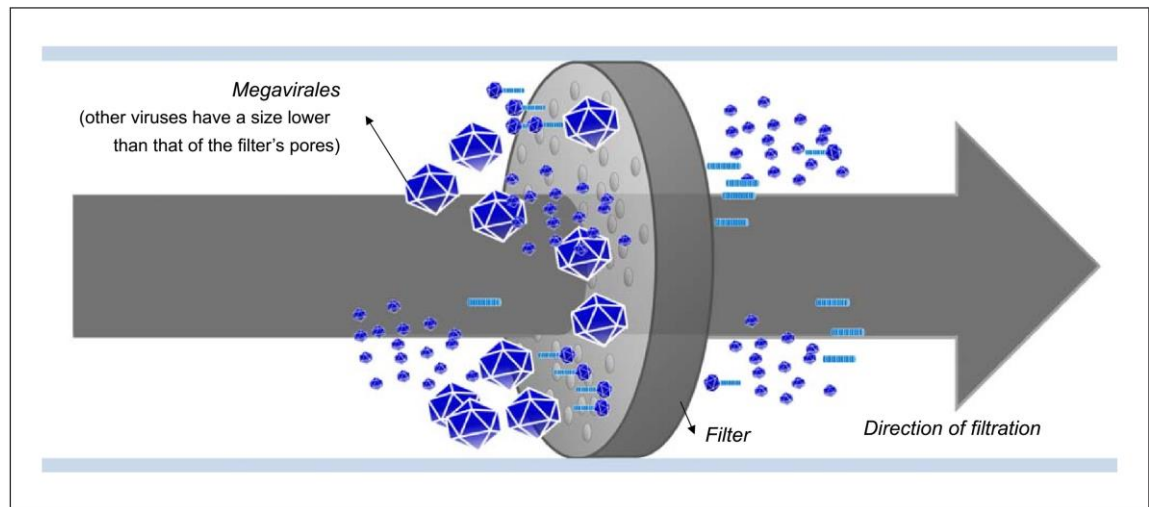


Figure 3. Filtering of samples have prevented viruses larger than the pore size (0.2- 0.45 μm) from getting detected (Colson et al. 2012).

2.2 Classification of Nucleocytoplasmic Large DNA Viruses:

Most of the giant viruses identified till now share a common ancestor with other viruses of the NCLDV group, which include viruses of the families Mimiviridae, Asfarviridae, Ascoviridae, Phycodnaviridae, Marseilleviridae, Iridoviridae and Poxviridae (Iyer et al. 2001) also recently discovered Pandaoraviruses (La Scola et al. 2003). The NCLDVs share a set of conserved genes which is considered the minimum genome for its ancestor, consequently the NCLDVs evolved, losing some of the genes as well as acquiring new genes from their hosts and other organisms they interact with (Yamada 2011). Gigantism of the genomes are only limited to Mimiviridae, Phycodnaviridae, Marseilleviridae lineages (Filée 2013).

Below is a table which lists the various NCLDVs and lists the respective genome sizes:

Table 1. NCLDV species, hosts and genome sizes (Filée 2013)

Major characteristics of completely sequenced NCLDV genomes.		
Virus name	Host name	Genome size (kb)
Mimiviridae		
Megavirus/Moumouvirus	<i>Acanthamoeba</i> sp.	1000–1259
Mamavirus/Mimivirus	<i>Acanthamoeba</i> sp.	1191–1182
CroV	<i>Cafeteria roenbergensis</i>	617
Phycodnaviridae		
EhVs	<i>Emilinia huxleyi</i>	407–410 (6 genomes)
Chlorella viruses	<i>Chlorella</i> sp.	288–369 (9 genomes)
ESV	<i>Ectocarpus siliculosus</i>	336
Prasinoviruses	Green alga	184–205 (8 genomes)
Feldmania virus	<i>Feldmania</i> sp.	154
Marseilleviridae		
Marseillevirus	<i>Acanthamoeba</i> sp.	368
Lausannevirus	<i>Acanthamoeba</i> sp.	346
Iridoviridae		
Ascovirus	Insects	119–186 (4 genomes)
Invertebrate iridescent virus	Insects	191–212 (3 genomes)
Ranavirus	Amphibians	106–140 kb (4 genomes)
Fish Iridovirus	Fishes	102–186 (3 genomes)
Poxviridae		
Chordo Poxviruses	Vertebrates	134–360 (27 genomes)
Entomopoxviruses	Insects	228–307 (6 genomes)
Unclassified NCLDVs		
PgV	<i>Phaeocystis globosa</i>	453–460 (2 genomes)
OLPV	?	344

The members of the NCLDV family are seen to show a high amount of genome plasticity. There is a high amount of duplicated genes in these viruses also horizontal gene transfer may have played an important role in gene plasticity. NCLDVs are seen to exchange genes with their hosts. Mimivirus, Marseillevirus and Phycodnavirus contain a high proportion of bacterial genes, this might be due to the reason that the phylogenic protist hosts of mimivirus feeds on bacteria. Thus, within these organisms

there might exist, a ‘hot pot’ of genomes, leading to the formation of chimeric organisms or gene transfer or acquisition among organisms (Filée & Chandler 2010).

Below is a comparison of the seven families of NCLDV with respect to its genome size, GC content, coding density and the number of genes:

Table 2. Comparison of the genomes of different NCLDVs (Colson et al. 2012)

Family	Genome size, nt		GC content, %		% coding		Number of genes	
	min	max	min	max	min	max	min	max
<i>Ascoviridae</i>	102,653	119,343	29	55	79	92	99	110
<i>Asfarviridae</i>	170,101	170,101	38	38	87	87	151	151
<i>Poxviridae</i>	134,431	359,853	17	64	80	96	130	328
<i>Marseilleviridae</i>	346,754	368,454	42	44	83	92	444	457
<i>Iridoviridae</i>	102,653	212,482	27	55	67	93	95	463
<i>Phycodnaviridae</i>	154,641	407,339	37	51	70	94	150	886
<i>Mimiviridae</i>	617,453	1,259,197	23	28	88	91	544	1,120

Recently a new classification system was proposed, which classified all organisms as either ribosome encoding organisms (Eukarya, Bacteria and Archea) or capsid encoding organisms like viruses (Forterre 2010) (Raoult & Forterre 2008) (Fig 3).

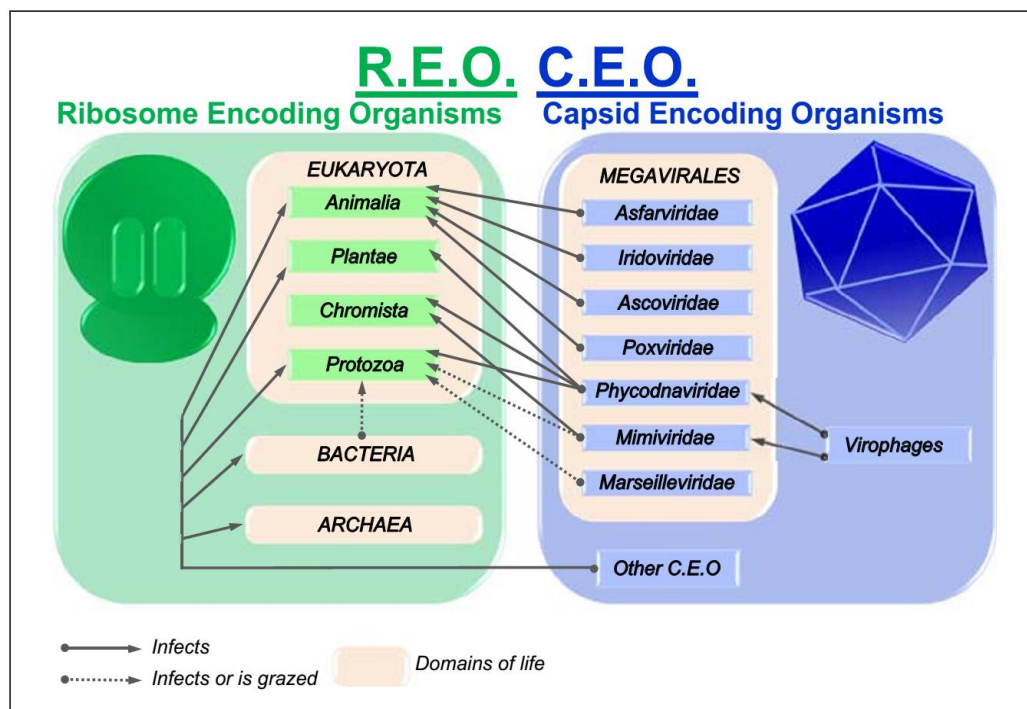


Figure 4. Proposed reclassification of organisms (Colson et al. 2012)

2.3 *Acanthamoeba polyphaga mimivirus*:

Discovery

In 1992, following a pneumonia outbreak in a study was being carried out to identify pneumonia causing organisms. An microorganism was isolated from the water of a cooling tower in Bradford, England. This microorganism resembled a small gram positive coccus under the light microscope (La Scola et al. 2003). Efforts to identify this microorganism was proving to be difficult, despite repeated attempts to amplify its 16s rRNA sequence using universal 16s rDNA bacterial primers there was no amplification result. When this organism was studied within *Acanthamoeba polyphaga*, electron microscopy revealed that it has a characteristic viral morphology. with the particle size being 400 nm in diameter and the capsid having a distinct icosahedral symmetry. It did not have an envelope but it had 80 nm fibrils attached to the capsid (Abrahão et al. 2014) (La Scola et al. 2005).

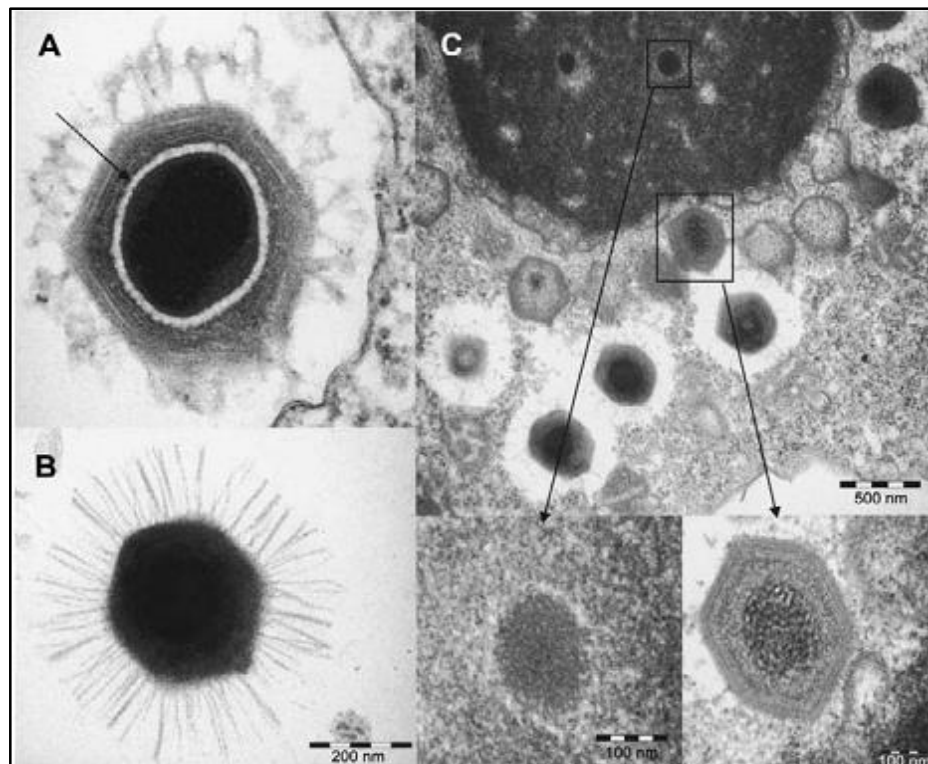


Figure 5. (A) Transmission Electron Microscopy showing viral particles in phagocytosis vesicles. (B) Mature Mimivirus particle with fibrils. (C) Dense core interpreted as viral factories (Raoult et al. 2007)

It was named Mimivirus (mimicking Microbe), since it resembled a bacterium during Gram staining. Preliminary assessment of its genome size revealed that it had a genome size ~800 kbp which was larger than several bacterial genomes.

Mimivirus was proposed to be a virus on the basis of the following characteristics (Suzan-Monti et al. 2006):

- i. Icosahedral structure.
- ii. Presence of a typical viral eclipse phase in its replication.
- iii. Lack of universal bacterial genes like ribosomal RNA and energy metabolism.
- iv. A high fraction of open reading frames which have no similarity to other organisms.
- v. Presence of genes which are homologous to proteins conserved in most NCLDV's (Table 3).

On the basis of these characteristics, Mimivirus was proposed to be a virus belonging to a new family of NCLDV group, known as Mimiviridae.

Table 3. NCLDV core genes found in Mimivirus

ORF no.	<i>Phycodnaviridae</i>	<i>Poxviridae</i>	<i>Iridoviridae</i>	<i>Asfarviridae</i>	Gene group	Definition/putative function (5)
L206	X	X	■	X	I	Helicase III / VV D5-type ATPase
R322	■	X	X	X	I	DNA polymerase (B family)
L437	X	X	■	X	I	VV A32 virion packaging ATPase
L396	■	X	x	X	I	VV A18 helicase
L425	■	X	X	X	I	Capsid protein D13L (4 paralogs)
R596	■	X	X	X	I	Thiol oxidoreductase (e.g., E10R)
R350	X	■	X	X	I	VV D6R helicase, +1paralog
R400	■	X	X	X	I	S/T protein kinase (e.g., F10L)
R450	■	X	X	X	I	Transcription factor (e.g., A1L)
R339	■x	X	X	X	II	TFII-like transcription factor
L524	x	X	■X	X	II	MuT-like NTP pyrophosphohydrolase
L323	x	X	■X	X	II	Myristoylated virion protein A
R493	■X	x	X	X	II	PCNA + 1 paralog
R313	X	■x	X	X	II	Ribonucleotide reductase, large sub.
L312	X	■x	X	X	II	Ribonucleotide reductase, small sub.
Not found	x	x	X	X	II	Thymidylate kinase
Not found	x	X	X	X	II	dUTPase
R429	■	—	X	X	III	PBCV1-A494R-like (9 paralogs)
L37	X	■	X	X	III	BroA, Kila-N term
R382	X	X	—	■	III	mRNA-capping enzyme
L244	—	X	■	X	III	RNA polymerase subunit 2 (Rbp2)
R501	—	X	■	X	III	RNA polymerase largest sub. (Rpb1)
R195	■	X	X	—	III	Glutaredoxin (e.g., ESV128)
R622	X	■	X	—	III	Dual spec. S/Y phosphatase
R311	—	x	X	X	III	BIR domain (e.g., CIV193R)
L65	—	■X	X	X	III	Virion-associated membrane protein
R480	■	—	X	X	III	Topoisomerase II
L364	X	■	X	—	III	SWI1/SNF2 helicase (e.g., MSV224)
Not found	x	X	X	—	III	RuvC-like HJR (e.g., A22R)
Not found	x	x	—	X	III	ATP-dependent DNA ligase (e.g., A50R)
Not found	—	x	X	X	III	RNA polymerase subunit 10

2.3.1 Mimivirus Genome

Mimivirus is one of the largest viruses characterized and it has a genome 1.2 Mb in size. Analysis of the sequence revealed 1262 open reading frames (ORFs), based on sequence alignment and homology 911 of these ORFs were predicted to encode proteins. Mimivirus shows a coding density of 90.5% (Raoult et al. 2004). Mimivirus is different from other large complex viruses as it is armed with a large arsenal of genes which are unique in the viral world, and until now only considered to be a part of the genomes of cellular organisms. These unique genes can be classified into four categories, which are – protein translation, DNA repair, molecular chaperones and enzymes for metabolic and other pathways (Raoult et al. 2004) (Jeudy et al. 2012).

Table 4. Mimivirus genes with their putative functions

ORF no.	Definition/putative function	Comment
R663	Arginyl-tRNA synthetase	Translation
L124	Tyrosyl-tRNA synthetase	Translation
L164	Cysteinyl-tRNA synthetase	Translation
R639	Methionyl tRNA synthetase	Translation
R726	Peptide chain release factor eRF1	Translation
R624	GTP-binding elongation factor eF-Tu	Translation
R464	Translation initiation factor SUI1	Translation
L496	Translation initiation factor 4E (mRNA cap binding)	Translation
R405	tRNA (Uracil-5-)-methyltransferase	tRNA modification
L359	DNA mismatch repair ATPase MutS	DNA repair
R693	Methylated-DNA-protein-cysteine methyltransferase	DNA repair
R406	Alkylated DNA repair	DNA repair
L687	Endonuclease for the repair of UV-irradiated DNA	DNA repair
L315 L720	Hydrolysis of DNA containing ring-opened N7-methylguanine	DNA repair
R194 R480 L221	Topoisomerase I pox-like, topoisomerase II, topoisomerase I bacterial type	DNA accessibility
L254 L393	Heat shock 70-kD	Chaperonin
L605	Peptidylprolyl isomerase	Chaperonin
L251	Lon domain protease	Chaperonin
R418	NDK synthesis of nucleoside triphosphates	Metabolism
R475	Asparagine synthase (glutamine hydrolyzing)	Metabolism
R565	Glutamine synthetase (Glutamate-amonia ligase)	Metabolism
L716	Glutamine amidotransferase domain	Metabolism
R689	N-acetylglucosamine-1-phosphate, uridylyltransferase	Polysaccharide synthesis
L136	Sugar transaminase, dTDP-4-amino-4,6-dideoxyglucose biosynthesis	ExoPolysaccharide synthesis
L780	dTDP-4-dehydrorhamnose reductase	ExoPolysaccharide synthesis
L612	Mannose-6P isomerase	Glycosylation
L230	Procollagen-lysine,2-oxoglutarate 5-dioxygenase	Glycosylation, capsid structure
L543	ADP-ribosyltransferase (DraT)	?
L906	Cholinesterase	Host infection?
L808	Lanosterol 14- α -demethylase	Host infection?
R807	7-dehydrocholesterol reductase	Host infection?
R322	Intein insertion	In DNA polymerase B

Along with the above genes Mimivirus also encodes for four aminoacyl tRNA synthetases, and a tRNA modifying enzyme (tRNA (Uracil-5-)-methyltransferase). It encodes all three type of Topoisomerases – type IA, type IB and type II. It also contains enzymes involved in glutamine metabolism and biosynthesis of polysaccharides. Although, inspite of this repertoire for genes within its genome, and its existence as an intracellular parasite these characteristics distinguish Mimivirus from intracellular bacteria (Yamada 2011) (Abergel et al. 2005) :

1. Mimivirus does not undergo division, and are assembled out of preformed components (Mutsafi et al. 2010).
2. Mimivirus does not encode for a ribosomal protein synthesis machinery and it cannot produce its own biological ATP (Yamada 2011) (Suzan-Monti et al. 2006).

2.3.2 Mechanism of replication in Mimivirus

Replication in Mimivirus

Replication is an essential part of the life cycle of every organism. The exact mechanism of replication in *Acanthamoeba polyphaga mimivirus* (APMV) is not fully characterized. Replication in Mimivirus typically follows an eclipse phase cycle, in which virions cannot be observed. DNA replication mainly occurs in the cytoplasm, independent of the host nucleus.

Virus entry and genome release

Mimivirus infection begins by the phagocytosis of virions by amoeba, phagocytosis occurs to be mediated by actin protrusions on the surface of the virus. Once the virion is successfully internalized and localized, the virus releases its genome by the formation of a star shaped structure on one of its vertices, this structure is named as 'stargate' (Zauberman et al. 2008). The stargate is centred at one of the vertices of the icosahedral structure and proceeds along its edges, with its appearance the genome gets pushed through towards the membrane of the phagosome followed by membrane fusion. Opening of the stargate might be due to action of lysozymes, as multiple lysosomes were seen to fuse with the phagosome (Zauberman et al. 2008). Similar mechanism has been seen to occur in *M. chilensis*, whereas in the newly discovered Pandoravirus and Pithovirus a cork like appearance is seen, unplugging of the cork occurs by a yet uncharacterized mechanism leading to ejection of genomic material (Legendre et al. 2014). It is to be noted that the naked genomic material cannot move through the dense cytoplasmic content without any kind of active transport system due to the dense nature of the cytoplasm (Mutsa et al. 2014).

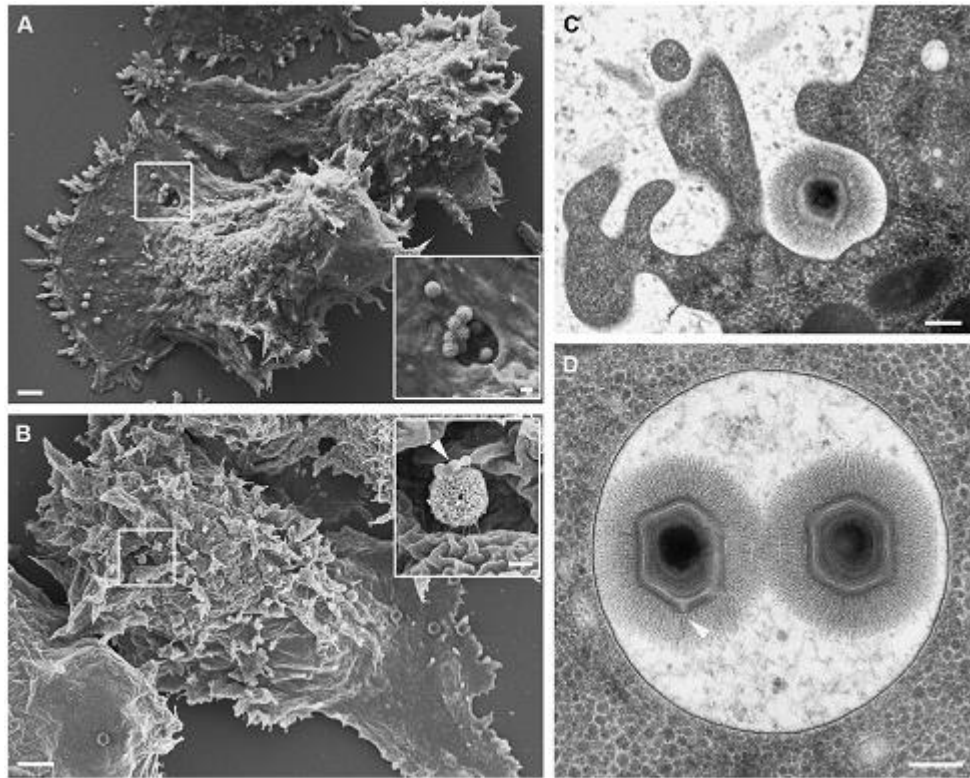


Figure 6. (A, B and C) Engulfment of virions by the host by phagocytosis. (D) Appearance of a stargate at the vertex (white arrow) (Zauberman et al. 2008).

Genome Replication and formation of Viral Factories

The viral genome is released as encapsulated cores after the opening of the stargate. These cores transport the genome to various sites in the cytoplasm. Followed by initiation of replication of the genome, thus creating replication centres. These replication centres join to form a viral factory which can assemble mature virions. These are seen after 7.5 hrs post infection by recruitment of the host cell membrane cisternae which are necessary for the formation of the viral factory (Mutsafi et al. 2013). The viral factory formed represent highly organized organelles, with the ability to generate multiple copies of viral progeny. Viral factories were suggested to be an actual living stage for the viruses (Claverie, 2006).

This process of replication is quite similar to the process in vaccinia virus.

Icosahedral capsids formation is initiated by the formation of a layer on top of the membrane and the emergence of angular surfaces (Fig 5). These surfaces expand to form the icosahedral capsids, immunolabelling assays suggest that the hypothetical mimivirus capsid protein L425 plays an important role in the assembly of the capsid.

This protein reveals similarity to the protein D13 from Vaccinia virus which is a capsid protein and plays a role as the scaffold in the formation of a viral capsid. But contrary to D13, L425 also appears to be a part of the mature virus.(Mutsafi et al. 2013)

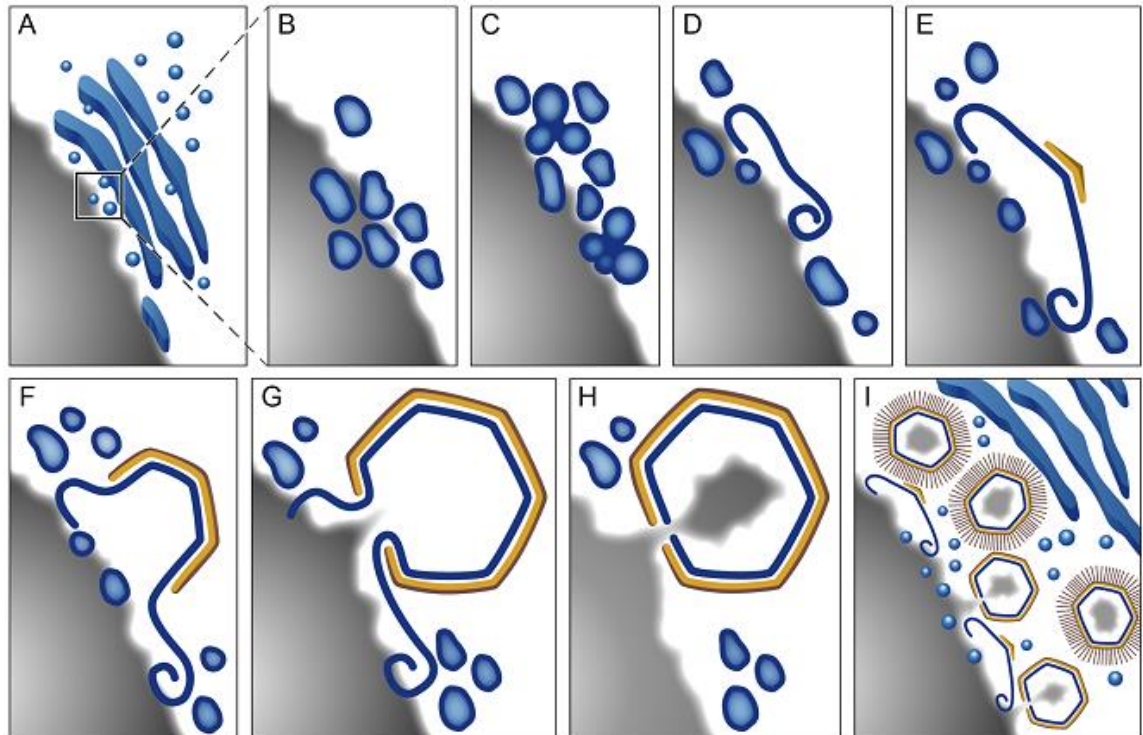


Figure 7. (A) Host Cisternae in the formation of early viral factories. (B) Multiple vesicles fuse together. (C) (D) Supervesicles formed open up 8hrs post infection to form the inner viral membrane. (E) Initiation of capsid formation. (F) Capsid formation. (G) (H) Membrane overhang to prevent premature closing of capsid. (I) Packaging and release of mature virions. (Mutsafi et al. 2013)

Replication system reminiscent of Poxviridae?

The replication of Mimiviridae and Poxviridae occurs in the cytoplasm in its entirety, unlike Phycodnavirus and Pandoraviruses which carry out their replication in the host nucleus. The nucleus associated replication of Phycodnavirus and Pandoravirus is due to their lack of essential replication related genes. Phylogenetic analysis place Mimiviridae between Iridoviridae and Phycodnaviridae, but the actual replication cycle observed resembles closely with Poxviridae (Mutsa et al. 2014) (Benarroch & Shuman 2006). Complete characterization of the replication system in Mimivirus is required so as to arm us with the necessary information needed to comment on the evolutionary similarity of the replicative mechanism to other organisms.

3.1 Primases

Replication of DNA is one of the most important process in cellular organisms as well as viruses. Many replicative proteins work together to carry out the process of replication, some of them being helicases – to unwind the DNA, topoisomerases – to relieve the topological stress, primase – to generate RNA primers. DNA polymerase carries out bulk of this work of synthesis of the DNA strand by adding nucleotides complimentary to the single strand (Boudet et al. 2015). In most characterized DNA replication systems, most DNA polymerases cannot start strand synthesis de novo it only extends existing stands, initiation of DNA replication requires a free 3' hydroxyl group to which dNTPs are added by DNA polymerase for novel strand synthesis (Lee et al. 2006).

Various mechanisms are employed by different organisms for priming (Iyer et al. 2005) (Desogus et al. 1999) (Crute et al. 1989) :

1. Cellular life forms, DNA viruses, Phages and Plasmids use a primase to synthesize a short RNA primer with a 3' OH group which is used by DNA polymerase to extend strand synthesis. Primase is a type of RNA polymerase that generates short RNA primers.

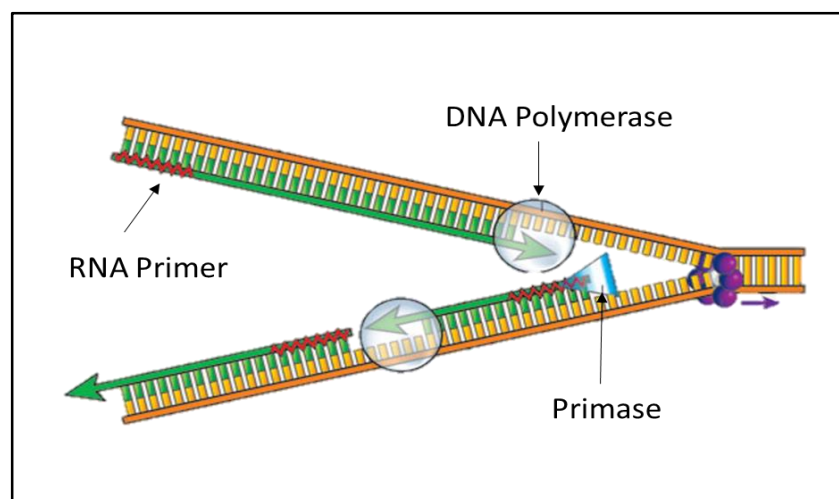


Figure 8. DNA polymerase extending strand synthesis from an RNA primer (Modified from Bell, 2006).

2. Retroviruses use a tRNA which primes DNA replication by providing a free 3' OH for Reverse Transcriptase to extend.

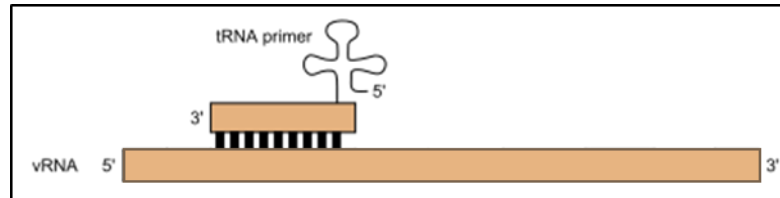


Figure 9. tRNA priming for Reverse Transcriptase (Modified from Filip Em, 2008)

3. In adenovirus and $\phi 29$ family of bacteriophages, the free 3' OH group is provided by the side chain of an amino acid of the terminal protein which is used by DNA polymerase to extend the strand.

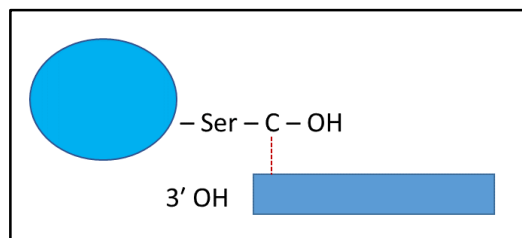


Figure 10. Protein Priming mechanism

4. Several DNA viruses, such as parvoviruses, circoviruses, phages and plasmids adopt a rolling circle mechanism for replication. In which an endonuclease makes a nick in one of the DNA strands. The 3' OH group thus freed is used by DNA polymerase for strand extension.

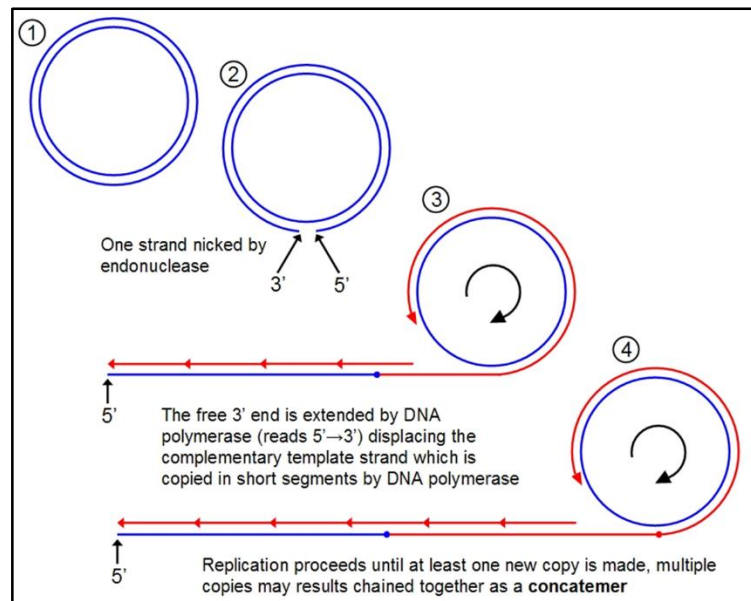


Figure 11. Rolling Circle replication mechanism (Anon, n. d.)

5. Some novel archaeal replicases harbour both DNA polymerase and Primase activities, also preferring dNTPs over rNTPs. Thus, enabling the polymerase to start replication *de novo* (Lipps et al. 2004).

3.1.1 Types of Primases

Primases are required for the replication of DNA in almost all cellular organisms and viruses, but there are two types of primases that function to produce primers:

i. In bacterial systems, the primase which is involved in replication belongs to the DnaG superfamily and it has the TOPRIM fold in its catalytic site (Iyer et al. 2005). The TOPRIM scaffold is also seen in topoisomerase Ia and topoisomerase II, OLD-family nucleases and RecR repair proteins.

ii. Whereas in archaeo-eukaryotic organisms, the primase involved in DNA replication contains a RRM (RNA recognition motif) fold (Boudet et al. 2015). RRM like scaffolds are found in RNA polymerases, Reverse Transcriptases, cyclic nucleotide generating cyclases and DNA polymerases which have a role in replication and repair.

Primases are one among many proteins of the archaeo-eukaryotic and bacterial lineages which are fundamentally different. The other proteins which are non-

homologous include the replicative polymerase, gap filling polymerase also the helicases involved in replication are non-orthologous between these lineages. But on the contrary, many of the other replicative proteins like DNA ligases, PCNA, clamp loader ATPases, Topoisomerase Ia and RNase HII are orthologous among archaeo-eukaryotic organisms and bacteria (Aravind et al. 1998). Study of the various proteins containing the TOPRIM domain has allowed us to understand the evolution of replication systems. The TOPRIM domain of DnaG is also found in the archaeal DnaG ortholog, and in topoisomerase Ia and topoisomerase II which are present across archaea and bacteria. Thus, this proves that replicative proteins with the TOPRIM architecture were already present in Last Universal Common Ancestor (LUCA). DnaG in archaea is also involved in RNA degrading exosome complex, so it is unclear if its role in LUCA was DNA repair or RNA metabolism (Iyer et al. 2005) (Forterre 2011).

Primases of the archaeo eukaryotic type, the Archaeo Eukaryotic Primases (AEP) have a more unclear origin. Members of the AEP superfamily were detected in various archaea (Gill et al. 2014). Here, they function in association with Ku protein, ATP dependent DNA ligases, and repair proteins involved in non-homologous end joining (NHEJ). Phylogenetic studies show that AEPs are a recent acquisition for archaea, also in the archaeo eukaryotic lineage AEPs evolved at the base of the tree. Thus, they were not a part of the replication system of LUCA (Iyer et al. 2005).

iii. A new family of AEPs known as the prim-pols have been described (García-Gómez S et al. 2013). They catalyse both DNA polymerase and RNA primase activity. They are often fused to Superfamily III helicases, or are encoded by genes neighbouring helicases. These helicases and the primase have been proposed to form the replication initiation complex of the ancestral plasmids. Their crystal structure showed that they shared structure with AEPs, thus that they are members of the AEP superfamily. The RRM motif consists of a highly conserved triad of acidic residues and a histidine residue. These residues have a conserved acidic and a histidine residue. These are involved in nucleotide binding and two metal ion catalytic mechanism, with either magnesium or manganese as cofactor (Boudet et al. 2015).

3.1.2 Mechanism of Primer synthesis

Studies on the biochemistry of the protein have been carried out on a macromolecular level to characterize the protein functionally. There are four basic steps involved in

primer synthesis: NTP binding, template binding, di-nucleotide formation and repositioning of the enzyme for primer extension (Boudet et al. 2015).

The synthesis of primers occurs on specific sequences on the template. Previous studies have shown that, in vitro, eukaryotic primases have only minimal specificity requirements, and a preference for pyrimidine rich templates (Boudet et al. 2015). However in vivo, the priming site specificity appears to not be so strict possibly due to the action of various proteins which are involved in this process. Some of the archaeal primases initiate primer synthesis at specific tri nucleotide sequences in the template. The nucleotide 5' on the tri nucleotide is often a cryptic nucleotide (Ramirez-Aguilar & Kuchta 2004). Also the concentration of rNTPs may have a role in the selection of priming site (Ramirez-Aguilar et al. 2002).

Kinetically it is proposed to be a two-step reaction, formation of the first phosphodiester bond followed by elongation of the primer. This requires the primase to contain two distinct nucleotide binding sites. The first step involves formation of the dinucleotide (Copeland & Wang 1993) then the primase moves, hydrolysis incoming nucleotides and adds them to the 3' end of the primer resulting in elongation. Zinc binding motif found in bacteriophage T7 primase-helicase is found to be important for the tri-nucleotide sequence recognition (Ichardson 1999) (Lee et al. 2012).

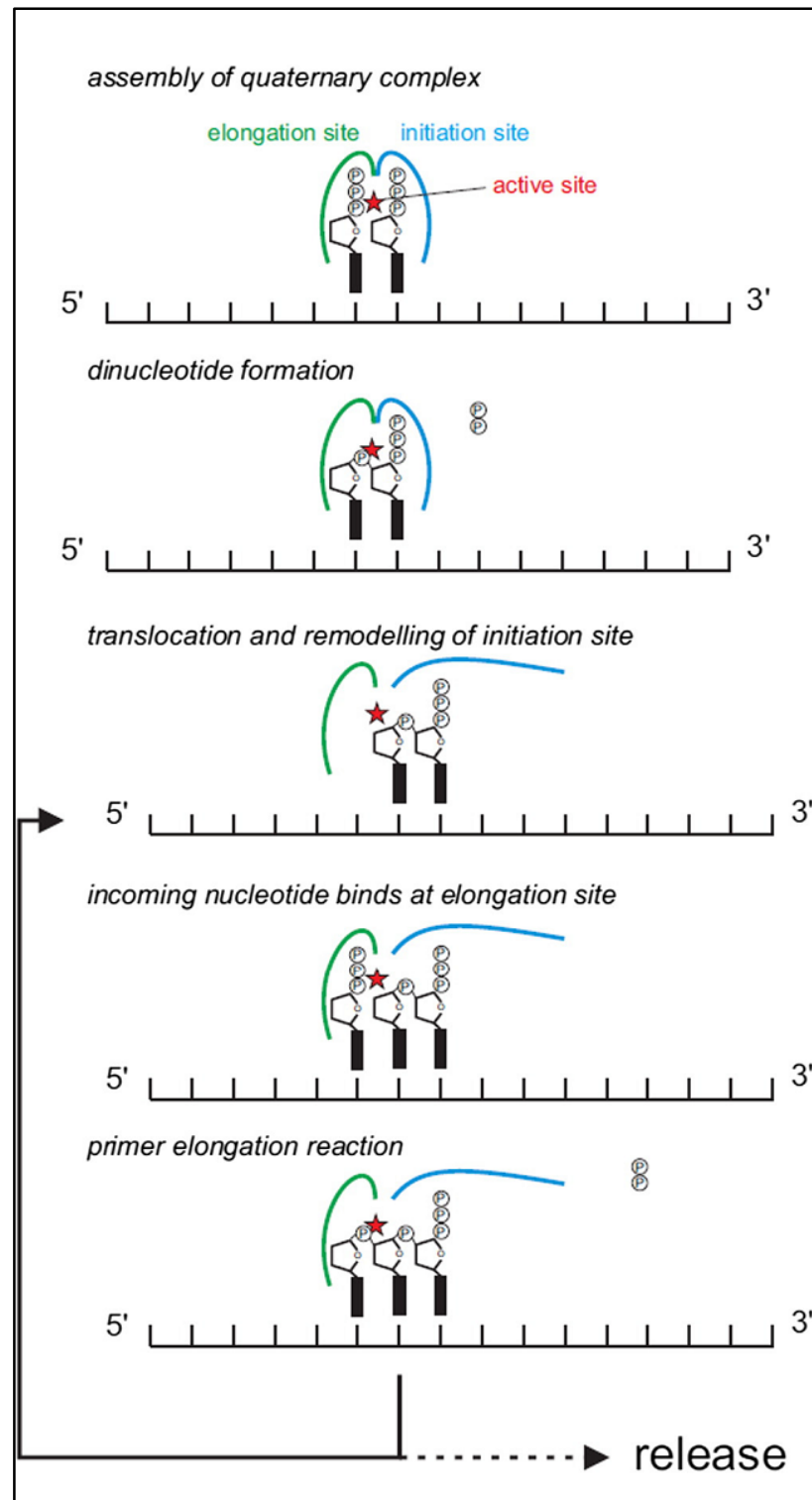


Figure 12. Mechanism of assembly of a quaternary complex of the primase-template and the first two nucleotides (Boudet et al. 2015)

CHAPTER 3

MATERIALS AND METHODS

3.1 Expression and Purification of wild type L537 protein from *Acanthamoeba polyphaga mimivirus*

3.1.1 Inoculation of Starter Culture

Materials:

1. Luria Broth
2. Chloramphenicol Stock (32 mg/ml)
3. Kanamycin Stock (10 mg/ml)
4. Primary Culture pET28b-L537 *Escherichia coli* BL21 RIPL cells.

Procedure:

1. 5ml sterile Luria Broth was taken in 4 test tubes and antibiotics Kanamycin and Chloramphenicol were added to it according to Table 1.
2. *E. coli* pET28b transformed RIPL cells were picked and inoculated in 4 test tubes containing 5ml Luria Broth.
3. The test tube was incubated overnight at 37°C in a shaker incubator at 250 rpm.

Table 5. Antibiotic Stock and Working Concentrations

Antibiotics	Stringent	Relaxed	Stock Solution	5ml culture
	Working			Working
Chloramphenicol	25 µg/ml	170 µg/ml	34 mg/ml in ethanol	3.67 µl
Kanamycin	10 µg/ml	50 µg/ml	10 mg/ml in H ₂ O	5 µl

3.1.2 Induction of Protein Expression

Materials:

1. Luria Broth
2. Chloramphenicol Stock (34mg/ml)
3. Kanamycin Stock (10mg/ml)
4. IPTG Stock (1M)
5. Autoclavable Low Speed Centrifuge Bottles

Procedure:

1. 2 litres of Luria Broth was inoculated with 1% v/v of overnight culture. The flask was incubated at 37°C in a shaker incubator at 250 rpm.
2. Antibiotics Kanamycin and Chloramphenicol were added according to Table 5.
3. The cells were allowed to grow till it reaches an Optical Density of 0.6 at 600 nm.
4. 1M IPTG was added to the culture to make a final concentration of 0.3mM (see Table 6).
5. The cultures were incubated at 30°C for 3 hours in a shaker incubator at 100 rpm.
6. After 3 hours cells were harvested in a centrifuge bottle by spinning at 4500 rpm for 10 mins at 4°C.
7. The pellet was stored at -80°C.

Table 6. IPTG Stock and Working Concentration

	Stock	Working (500ml culture)
IPTG	1 M	0.3 mM (150 µl)

3.1.3 Protein Purification

Materials:

1. Screw cap Oak Ridge Tubes
2. AKTA Start system (purchased from GE Healthcare Life Sciences)

3. Ni NTA pre packed column.
4. AKTA Purifier system (purchased from GE Healthcare Life Sciences)
5. Superdex™ 200 pg pre packed column.

Procedure:

3.1.3.1 Sample Preparation

1. The pellet was resuspended in 40 ml of Binding Buffer (0.5M NaCl, 50mM Tris HCl (pH 8.0), 5mM MgCl₂, 10mM Imidazole, 10% Glycerol) with 800ul of PMSF (8.7mg/ml) and 1mM Benzamidine Hydrochloride.
2. The suspension was sonicated for 15 mins (40% Amplitude, 2 second pulses, 2 second off).
3. The sonicated suspension was centrifuged at 12500 rpm for 20 mins at 4°C. The supernatant was collected.
4. Filter the supernatant using a 0.2μ filter.

3.1.3.2 Affinity Chromatography with pre packed Ni-NTA column on AKTA Start System

Column Equilibration

1. 10 CV (Column Volume) of Filtered Milli-Q water through all tubes, avoid passing air bubbles through the column.
2. 10 CV of Binding Buffer (see Appendix.) through the column.

Sample Application

1. The filtered supernatant was allowed to pass through the column, subsequently two washes were given at 3.33% elution buffer (10 CV) and 8.33% elution buffer (20 CV) to wash off non-specific proteins.
2. Percentage of Elution buffer (0.5M NaCl, 50mM Tris HCl (pH 8.0), 5mM MgCl₂, 600mM Imidazole, 10% Glycerol) was increased from 8.33% to 100% in 50 ml.
3. The flow through was collected and stored at -20°C for loading on SDS PAGE gel.

4. 0.5ml fractions were collected at the UV peak corresponding to the protein of interest.
5. The presence of protein in the fractions was verified running an SDS PAGE gel. Fractions which showed the band corresponding to the protein of interest were pooled and concentrated to 2 ml.

3.1.3.3 Size Exclusion Chromatography with pre packed Superdex™ 200 column on the AKTA Purifier System

Column Equilibration

1. The column was equilibrated by passing 2 CV of gel filtration buffer (0.5M NaCl, 50mM Tris HCl (pH 8.0), 1% glycerol).

Sample Application

1. A syringe was used to inject 2 ml of the pooled fraction into the system.
2. 0.5ml fractions were collected at the UV peak, and loaded on the SDS PAGE gel to verify the presence of protein.
3. Fractions which showed the band corresponding to the protein of interest were pooled and concentrated to 200 µl.
4. The concentrate was dispensed into 20 µl aliquots and stored at -80°C.

3.1.4 Estimation of Protein Concentration

3.1.4.1 Bradford Assay

Materials:

1. BSA Stock (1 mg/ml)
2. Bradford Reagent (see appendix)

Procedure:

1. BSA standard dilutions and a blank were prepared as given in Table 3.
2. 100 μ l of 1:100 and 1:50 dilutions of the protein were prepared.
3. 900 μ l of the Bradford reagent was added to all tubes, making the final volume to 1ml.
4. The tubes were incubated at room temperature for 10 mins.
5. Absorbance was measured at 595nm.

Table 7. BSA Dilutions.

Concentration of BSA (μ g)	Volume of BSA 0.1 mg/ml (μ l)	Volume of H ₂ O (μ l)
Blank	0	100
1	10	90
2	20	80
3	30	70
4	40	60
5	50	50
6	60	40
7	70	30
8	80	20
9	90	10

Table 8. L537 Dilutions

Concentration of L537	Volume of L537 (μl)	Volume of H ₂ O (μl)
1:100	1	99
1:50	2	98

3.1.4.2 Absorbance at 280 nm

Materials:

1. Gel Filtration Buffer

Procedure:

1. 1:10 dilution of the protein was prepared with the gel filtration buffer.
2. Absorbance was measured at 280 nm.

3.1.4.3 Estimation of Protein Concentration by ImageJ

Materials:

1. ImageJ Software
2. SDS PAGE apparatus
3. Gel Documentation System
4. BSA Stock (1mg/ml)

Procedure:

1. Dilutions of BSA and the protein to be quantified were prepared as shown in Table 4 and Table 5 respectively.
2. These were loaded on SDS Page Gel, and a gel image was captured.
3. The lanes were marked and the concentration of BSA was quantified using ImageJ.
4. A standard graph was plotted which was used to calculate the concentration of protein.

Table 9. Dilutions of BSA for ImageJ protein quantification

Concentration of BSA (μg)	Volume of BSA 0.1 mg/ml (μl)	Volume of H₂O (μl)
1	10	90
2	20	80
3	30	70
4	40	60
5	50	50

Table 10. L537 Dilutions for ImageJ protein quantification

Concentration of L537	Volume of L537 (μl)	Volume of H₂O (μl)
Neat	10	-

3.2 Introduction of H173A mutation in L537 gene from Mimivirus

3.2.1 Cloning of L537 gene with H173A mutation in *E. coli* DH5 α cell

3.2.1.1 DpnI Digestion of PCR product to remove template plasmid

Materials:

1. DpnI
2. DpnI Buffer
3. Nuclease free H₂O

Procedure:

DpnI digestion:

1. 15 μ l of PCR product was taken and 1 μ l of DpnI, 2 μ l of buffer, 2 μ l nuclease free H₂O were added to it.
2. The mixture was incubated at 37°C for 1 hour.
3. The enzyme was heat inactivated by heating at 65°C for 15 mins.

3.2.1.2 *E. coli* DH5 α competent cell preparation:

Materials:

1. Test Tube with 5ml sterile Luria Broth
2. 100ml of sterile Luria Broth
3. Autoclaved Oak Ridge culture tubes
4. 100mM CaCl₂
5. 85mM CaCl₂ with 15% glycerol

Procedure:

1. Test tube with Luria Broth was inoculated with DH5 α cells. The test tube was incubated at 37°C overnight.
2. 100ml of sterile Luria Broth was inoculated with 1ml of overnight culture of *E. coli* DH5 α cells.
3. The cells were allowed to grow till an Optical Density of 0.4 – 0.6 was reached.

4. The cells were harvested by spinning at 3000 rpm for 15 mins at 4°C.
5. The supernatant was discarded and the pellet was resuspended in 50ml of cold 100 mM CaCl₂.
6. It was incubated on ice 30 mins, followed by spinning at 3000 rpm for 15 mins at 4°C.
7. The supernatant was discarded and the pellet was resuspended in 5 ml of cold 85 mM CaCl₂ + 15% glycerol.
8. The cells were then aliquoted into sterile 1.5ml microcentrifuge tubes and stored at -80°C.

3.2.1.3 Transformation of H173A mutant L537 into DH5α competent cells by Heat Shock Method:

Materials:

1. 100 µl of *E. coli* DH5α competent cells
2. DpnI digested PCR product
3. Sterile Luria Broth

Procedure:

1. 100 µl of DH5α competent cells were thawed on ice, and 10µl of DpnI digested PCR product was added to it.
2. This mixture was incubated on ice for 45 mins.
3. After incubation, a heat shock was given to the mixture at 42°C for 90 seconds, leave on ice for 5 mins.
4. 900 µl of sterile LB was added to the tubes.
5. The cells were allowed to grow for 1 hour at 37°C.
6. Spin the tube at 8000 rpm for 2 mins. Discard 500µl of supernatant, and resuspend the pellet in the remaining media.
7. 100µl of cells were spread on plates containing selectable marker. Incubate the plates at 37°C for 12 – 16 hrs, till isolated colonies can be observed.
8. The plates were stored at 4°C.

3.2.2 Transformation of L537 gene with H173A mutation in *E. coli* BL21 RIPL cells

3.2.2.1 *E. coli* DH5 α Plasmid Preparation

Materials:

1. Alkaline Lysis solution I (see appendix)
2. Alkaline Lysis solution II (see appendix)
3. Alkaline Lysis solution III (see appendix)
4. Isopropanol
5. 80% Ethanol

Protocol:

1. *E. coli* DH5 α transformed colonies were picked and inoculated in tubes containing Luria Broth, and allowed to grow overnight.
2. 1ml of overnight culture was taken in 1.5ml micro centrifuge tubes, and centrifuged at 8000 rpm for 2 mins.
3. The supernatant was discarded and 200 μ l of cold Alkaline Lysis Solution I was added to the tubes, it was vortex to resuspend the pellet.
4. The tubes were left on ice for 10 mins.
5. 200 μ l of freshly prepared Alkaline Lysis Solution II was added to the tubes. It was mixed gently by inversion. Followed by incubation at room temperature for 5 mins.
6. 200 μ l of cold Alkaline Lysis Solution III was added to the tubes. It was mixed gently by inversion. Followed by incubation on ice for 15 mins.
7. The tubes were centrifuged at 14,000 rpm for 10 mins at 4°C.
8. The supernatant was carefully transferred to fresh tubes avoiding the precipitate.
9. 600 μ l of isopropanol was added to the tubes, mixed and allowed to stand at room temperature for 15 mins.
10. The tubes were centrifuged at 14,000 rpm for 10 mins at room temperature.
11. The supernatant was discarded and 500 μ l of 80% ethanol was added to the tubes.

12. The tubes were centrifuged at 14,000 rpm for 1 minute at 4°C, the supernatant was discarded and the pellet was allowed to air dry.
13. The pellet was resuspended in 20 µl of nuclease free water, and stored at 4°C.
14. The presence of the plasmid was verified by 0.8% Agarose Gel Electrophoresis.

3.2.2.2 *E. coli* BL21 RIPL competent cell preparation

Materials:

1. Test Tube with 5ml sterile Luria Broth
2. 100ml of sterile Luria Broth
3. Autoclaved Oak Ridge culture tubes
4. 100mM CaCl₂
5. 85mM CaCl₂ with 15% glycerol

Procedure:

1. Test tube with Luria Broth was inoculated with *E. coli* BL21 RIPL cells. The test tube was incubated at 37°C overnight.
2. 100ml of sterile Luria Broth was inoculated with 1ml of overnight culture of *E. coli* BL21 RIPL cells.
3. Procedure as given in 3.2.1.2 was followed.

3.2.2.3 Transformation of L537 gene with H173A mutation into *E. coli* BL21 RIPL cells by Heat Shock Method

Materials:

1. 100 µl of *E. coli* BL21 RIPL competent cells.
2. Purified Plasmid.
3. Sterile Luria Broth.

Procedure:

1. 100 µl of *E. coli* BL21 RIPL competent cells were thawed on ice, and 1 µl of isolated plasmid was added to it.

2. Procedure as given in 3.2.1.3 was followed

3.2.2.4 Preparation of Glycerol Stock

Materials:

1. 50% Glycerol

Procedure:

1. Test tube with Luria Broth was inoculated with transformed cells. The test tube was incubated at 37°C overnight.
2. 300 µl of 50% Glycerol and 700 µl of culture were taken, vortexed and stored at -80 °C.

3.3 Estimation of Primase Activity

3.3.1 Malachite Green Assay

For the detection of primase activity the method described by Biswas, Resto-Roldá N, Sawyer, Artsimovitch, & Tsodikov, 2013 was routinely used. The principle of this method involves the use of inorganic pyrophosphatase (PPiase) as a coupled enzyme. PPiase cleaves pyrophosphate (PPi) into two phosphates (Pi). Primase acts to add rNTPs on a single stranded DNA template. Addition of rNTPs is coupled with the release of a pyrophosphate. This is acted upon by PPiase to release phosphate, the phosphate thus released is detected by the interaction with Malachite Green Regent.

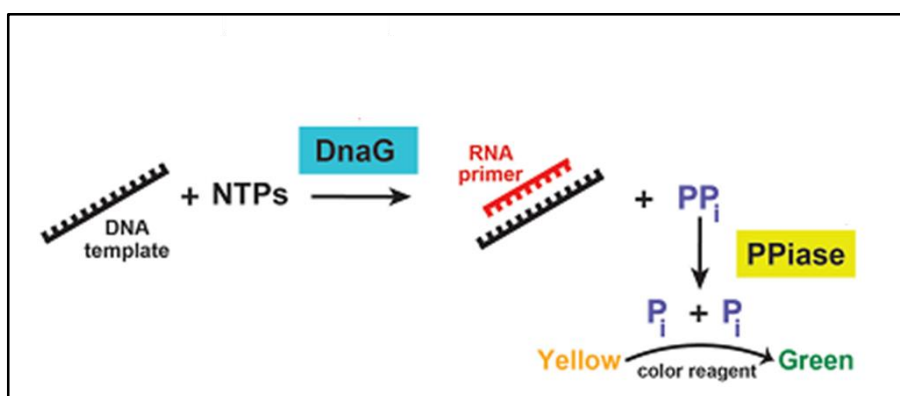


Figure 13. Principle of Primase- Pyrophosphatase assay (Modified from Biswas et al., 2013)

3.3.1.1 Preparation of Malachite Green Dye

Materials:

1. H_2SO_4 Stock
2. Malachite Green Dye
3. Ammonium Molybdate
4. Tween 20

Procedure:

1. 37N H_2SO_4 stock was diluted to 5N H_2SO_4 to make a final volume of 100ml. 0.14g of Malachite Green dye was added to it, to make Malachite Green solution.

2. On the day of use, 2.5 ml of 7.5 % Ammonium Molybdate was taken in a 15 ml Falcon tube.
3. 200 μ l of 11% Tween 20 was added to it.
4. The volume was made up to 10 ml by adding Malachite Green Solution.

3.3.1.2 Phosphate Standard Curve

Materials:

1. KH_2PO_4 Stock (0.1mM)
2. Malachite Green Dye

Procedure:

1. Dilutions of KH_2PO_4 were prepared according to the following table:

Table 11. Phosphate standard curve (Dilutions)

Concentration of Phosphate (μM)	Volume of KH_2PO_4 0.1 mM (μl)	Volume of H_2O (μl)
BLANK	0	800
1	10	790
2	20	780
3	30	770
4	40	760
5	50	750
6	60	740
7	70	730
8	80	720
9	90	710
10	100	700

1. 200 μ l of Malachite Green Dye was added to the tubes.
2. The tubes were incubated at room temperature for 30 mins.
3. The absorbance was checked at 630nm.

4. The absorbance was plotted against the concentration of phosphate to get the standard curve.

3.3.1.3 Primase Pyrophosphatase Assay

Materials:

1. rNTP Stock (10mM)
2. MgCl₂ (10mM)
3. Pyrophosphatase (100U/ml)
4. Template DNA

Procedure:

1. To check the primase activity of purified L537 protein, the following reagents were added to PCR tubes to make a final volume of 30 µl.
2. The various reagents were added according to the following table:

Table 12. Primase assay mix

Reagents	Stock Concentration	Working Concentration
L537	As Calculated	2 µM
rNTPs	10 mM	80 µM
MgCl₂	10 mM	1 mM
Template DNA	As Provided	3 µM
Pyrophosphatase	100U / ml	0.1 U

3. The volume was made up to 30 µl with Nuclease free H₂O.
4. The PCR tubes were incubated at 22°C for 30 mins in a Thermal Cycler.
5. The reaction was stopped by addition of 1mM EDTA.
6. The reaction product was transferred to 1.5 ml microcentrifuge tubes.
7. The volume was made up to 800 µl using H₂O, and 200 µl of Malachite Green Dye was added to the tubes.
8. The tubes were incubated at room temperature for 30 mins.
9. The absorbance was checked at 630nm.

CHAPTER 4

RESULTS

4.1 Purification of wild type L537 from *E. coli* BL21 RIPL cells

4.1.1 Induction of protein expression

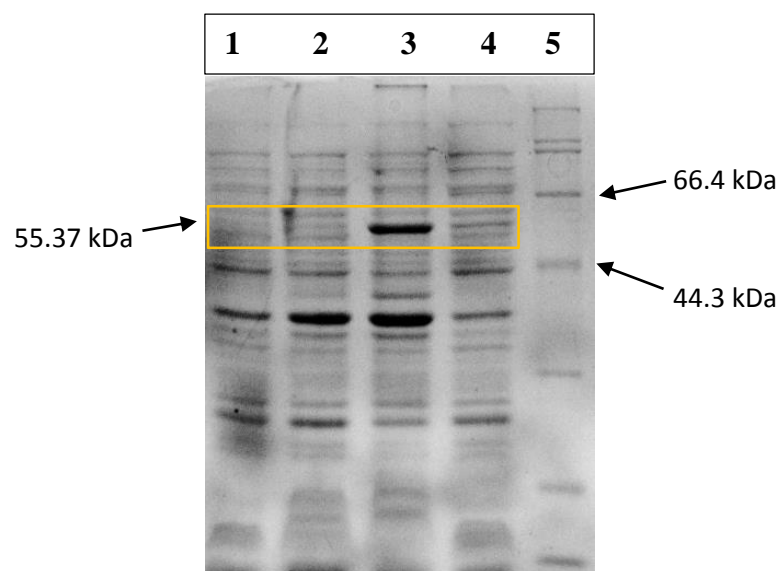


Figure 14. L537 induction at 30°C for 3 hours.

Lane 1	-IPTG
Lane 2	+IPTG
Lane 3	Pellet after Sonication
Lane 4	Supernatant after Sonication
Lane 5	Protein Ladder

4.1.2 Affinity Chromatography – Chromatogram

The sample for affinity chromatography was obtained after procedure 3.1.3.1.

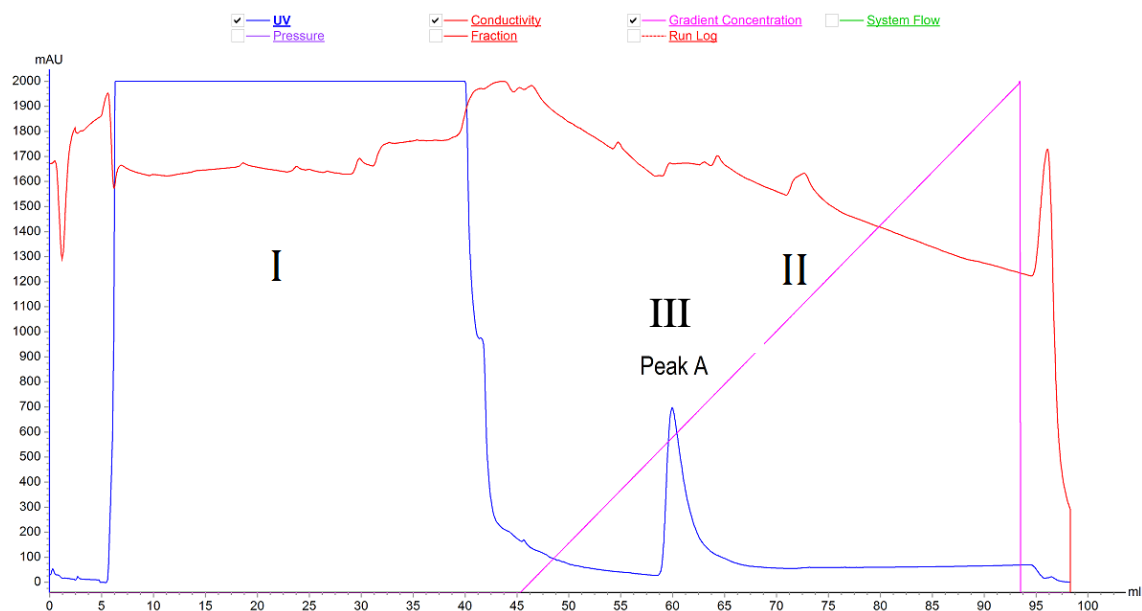


Figure 15. Affinity Chromatogram for WT L537. Refer Appendix for program details.

I – Flow Through

II – Imidazole gradient concentration

III – Peak A

A single sharp peak was observed at an imidazole concentration of ~ 60 mM. 0.5 ml fractions were collected in fraction collection tubes at Peak A , these fractions were loaded onto an SDS PAGE gel.

4.1.3 Affinity Chromatography – Fractions

For SDS PAGE gel composition and sample preparation protocol refer Appendix

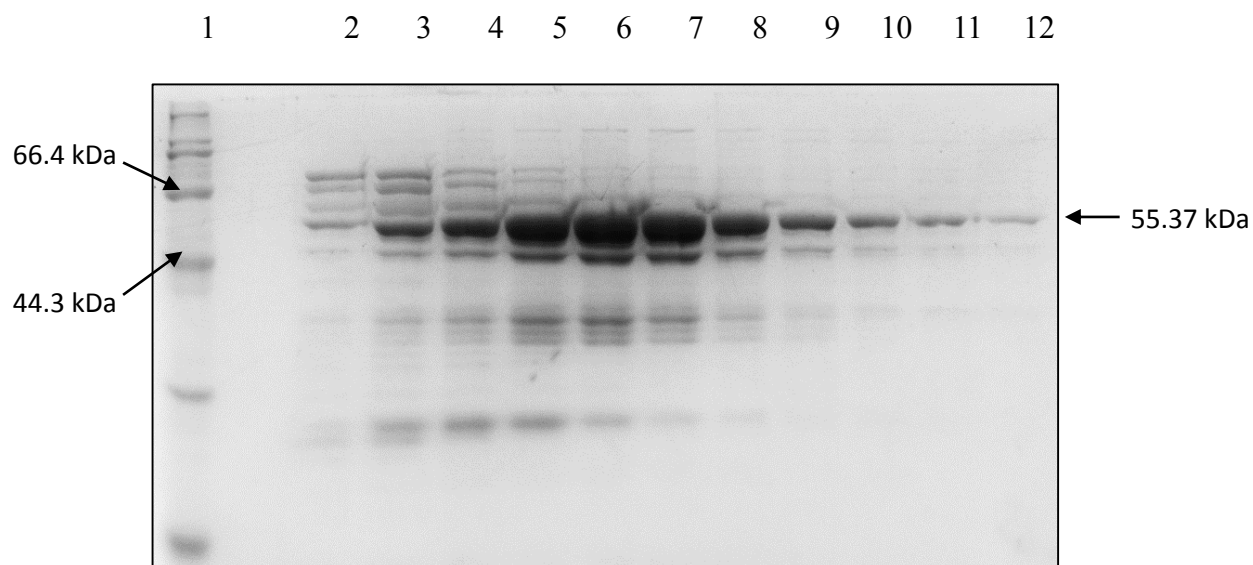


Figure 16. Affinity Chromatography Fractions (Peak A)

Lane 1	Protein Ladder
Lane 2	Fraction 1
Lane 3	Fraction 3
Lane 4	Fraction 5
Lane 5	Fraction 7
Lane 6	Fraction 9
Lane 7	Fraction 11
Lane 8	Fraction 13
Lane 9	Fraction 15
Lane 10	Fraction 17
Lane 11	Fraction 19
Lane 12	Fraction 21

A thick band was observed between the positions 66.4 kDa and 44.3 kDa.

The fractions that were relatively pure were selected and pooled for Size Exclusion Chromatography. Fractions 11 to 21 were pooled and concentrated to 2 ml.

4.1.4 Size Exclusion Chromatography – Chromatogram

Sample for Gel Filtration was obtained after procedure 3.1.3.2

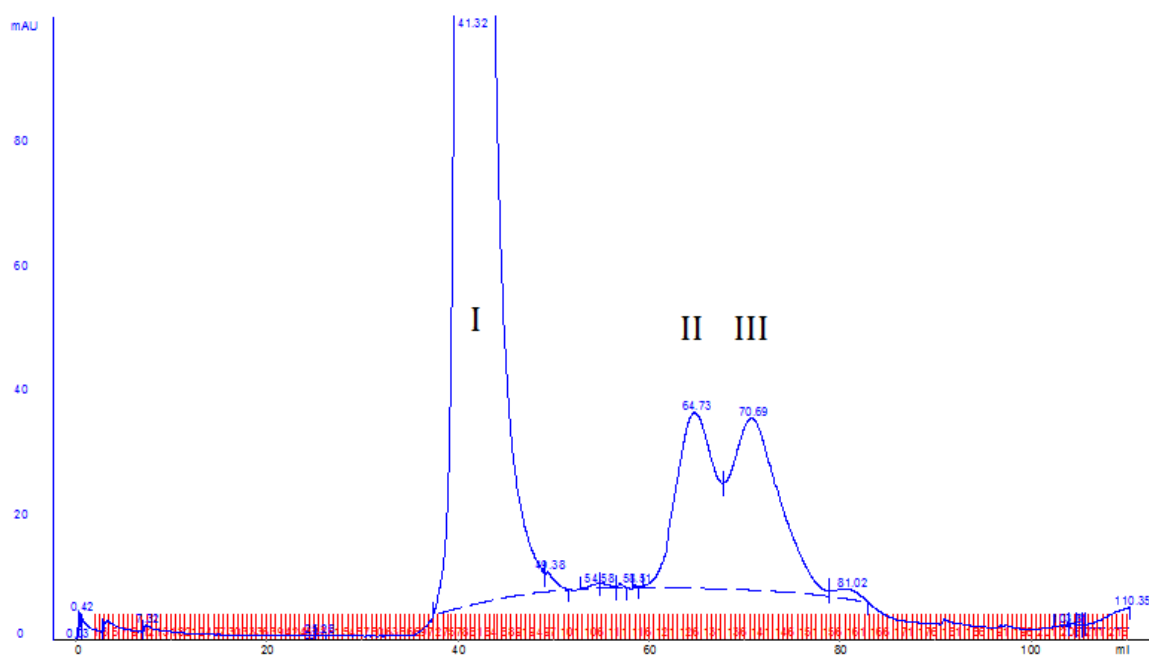


Figure 17. Size Exclusion Chromatography – Chromatogram. Refer Appendix for program details

I - Void Volume (41.32 ml)

II - Peak 1 (64.73 ml)

III - Peak 2 (70.69 ml)

Three peaks were observed, peak corresponding to void volume (V_o) was obtained at 41.32 ml, 0.5 ml fractions were collected at Peak I and Peak II and loaded onto an SDS PAGE gel.

4.1.5 Size Exclusion Chromatography – Fractions

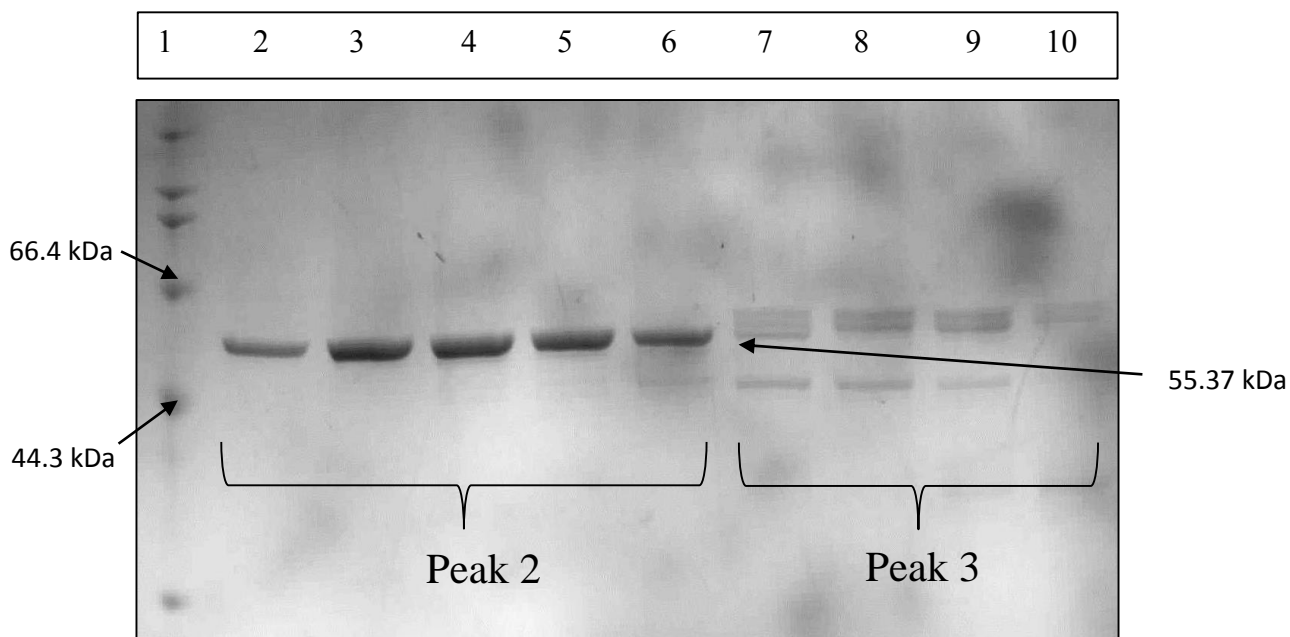


Figure 18. Size Exclusion Chromatography Fractions (II & III)

Lane 1	Protein Ladder	
Lane 2	Fraction 6	Peak 2
Lane 3	Fraction 9	
Lane 4	Fraction 11	
Lane 5	Fraction 13	
Lane 6	Fraction 15	
Lane 7	Fraction 19	Peak 3
Lane 8	Fraction 22	
Lane 9	Fraction 25	
Lane 10	Fraction 28	

L537 elutes at Peak 2 which is ~ 65ml. The fractions containing pure protein were pooled and concentrated to 250µl using a molecular weight cut-off concentrator.

4.1.6 L537 wild type – Purification Profile

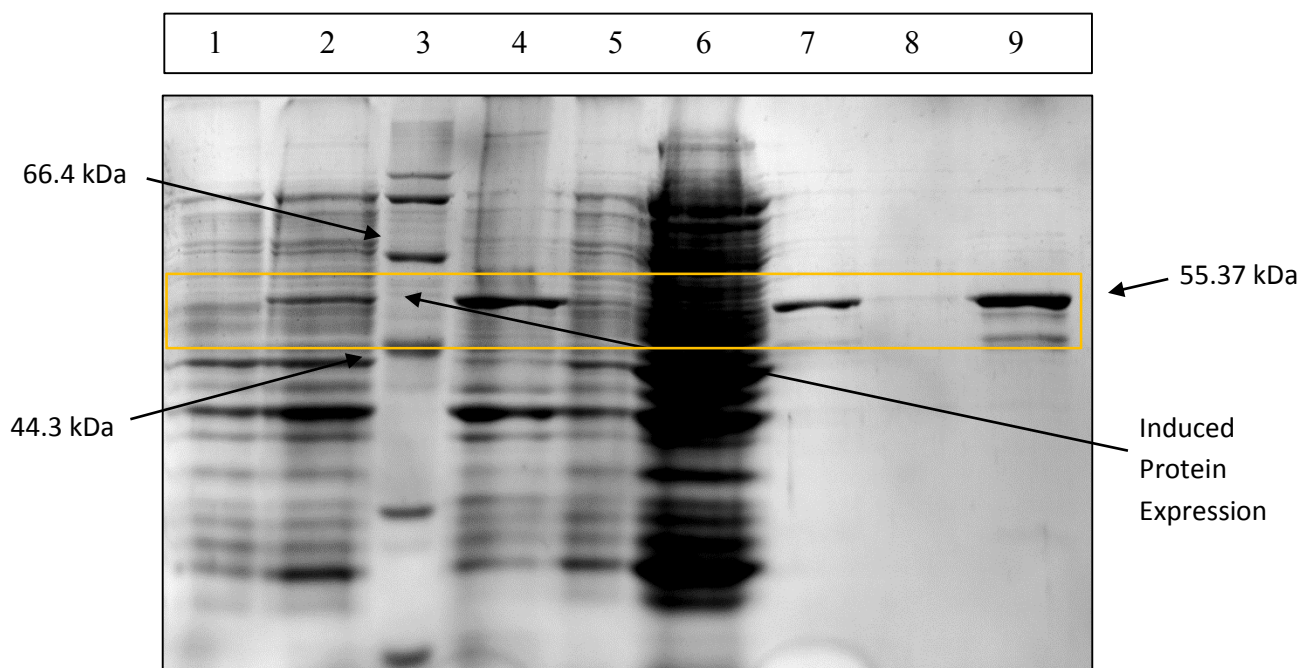


Figure 19. Purification profile of wild type L537

Lane 1	- IPTG
Lane 2	+ IPTG (3 Hour Induction)
Lane 3	Protein Ladder
Lane 4	Pellet after Sonication
Lane 5	Supernatant after Sonication
Lane 6	Affinity Flow Through
Lane 7	Affinity Purified
Lane 8	Void Volume
Lane 9	Purified Protein

4.1.7 Estimation of the Concentration of Purified Protein

4.1.7.1 Estimation of Concentration by Bradford Assay

Table 13. BSA standard curve

Concentration of BSA (μg)	Absorbance at 595nm *
BLANK	0
1	0.079
2	0.168
3	0.213
4	0.273
5	0.33
6	0.371
7	0.454
8	0.5
9	0.542

* Value taken was an average of two readings.

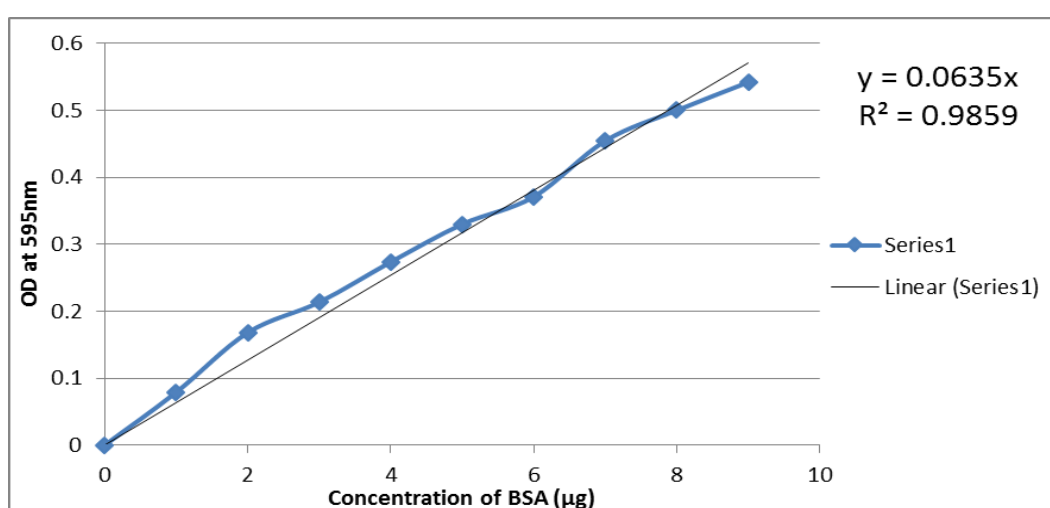


Figure 20. BSA Standard Curve

Table 14. L537 Dilutions for Bradford Assay

L537 Dilution	Absorbance _{avg} at 595nm *	L537 concentration (µg/ul)
1:100	0.16	2.51
1:50	0.331	2.60

* Value taken was an average of two readings.

From the BSA standard curve we get the equation for the slope, $y = 0.0635 x$.

$$x = \frac{y}{0.0635}$$

Thus, we calculated the concentrations of 1:100 and 1:50 dilutions as 2.51 µg/µl and 2.60 µg/µl.

$$\text{No of Moles} = \frac{2.55 \times 10^{-6}}{55880}$$

$$\text{Molar Concentration} = \frac{2.55 \times 10^{-6}}{55880 \times 10^{-6}}$$

Thus, Molar Concentration of the purified protein was calculated to be 45.63 µM.

4.1.7.2 Estimation of protein concentration by checking Absorbance at 280 nm

To verify the protein concentration, absorbance of the purified protein was checked at 280 nm. The sample was diluted according to procedure given in 3.1.4.2.

$$OD_{280} = 0.22 \times 10^*$$

*dilution factor

$$\begin{aligned}\text{Molar Concentration} &= \frac{\text{Absorbance}}{\text{Molar extinction coefficient } (\epsilon) \times \text{path length}} \\ &= \frac{2.2}{56645 \times (1)}\end{aligned}$$

where,

Molar extinction coefficient (ϵ) \rightarrow 56645 M⁻¹cm⁻¹ (from ExPASy ProtParam tool)

Path length \rightarrow 1 cm

Thus, the Molar Concentration of purified L537 was calculated to be 38.83 μ M.

Due to the variation in the protein concentration in Bradford assay and Absorbance at 280 nm, it was necessary to quantitate the protein using another method to verify the concentration of protein.

4.1.7.3 Estimation of protein concentration by Imaging

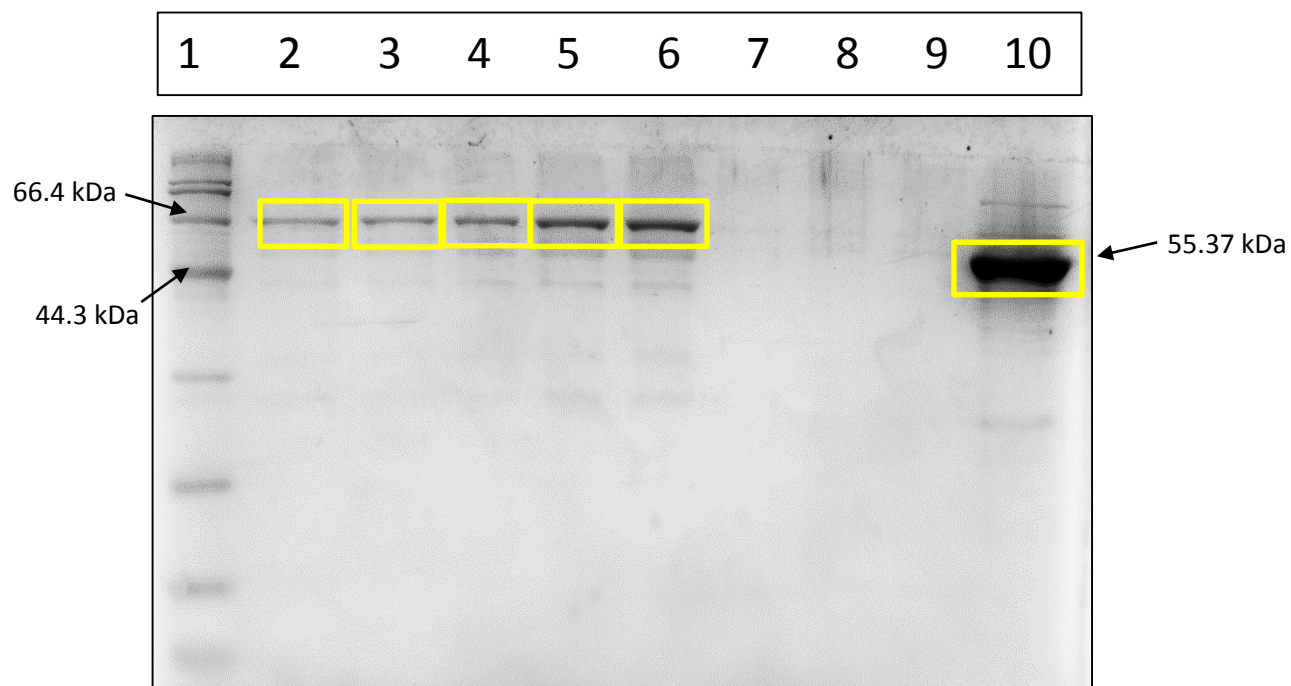


Figure 21. Protein concentration by Imaging

Lane 1	Protein Ladder
Lane 2	BSA 1 µg
Lane 3	BSA 2 µg
Lane 4	BSA 3 µg
Lane 5	BSA 4 µg
Lane 6	BSA 5 µg
Lane 10	L537 neat

Table 15. BSA Standard Pixel Density (ImageJ)

Concentration of BSA (μg)	Pixel Density
1	1070.205
2	2008.497
3	2880.74
4	4104.468
5	4910.296

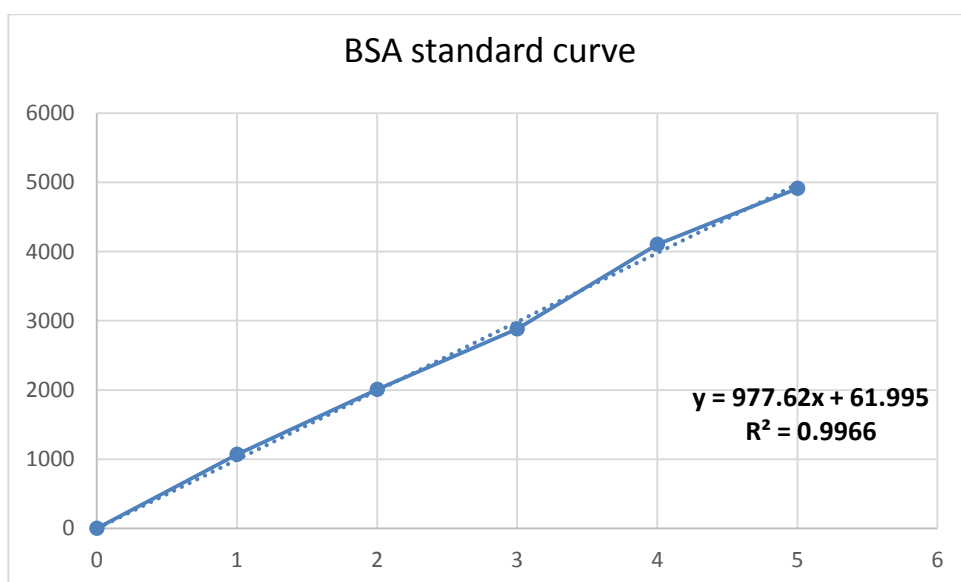


Figure 22. BSA Standard Curve (ImageJ)

$$\begin{aligned}
 \text{Concentration of Protein} &= \frac{25925.41 - 61.995}{977.64} \\
 &= 25.94 \mu\text{g}/10 \mu\text{l} \\
 &= 2.59 \mu\text{g}/\mu\text{l}
 \end{aligned}$$

$$\text{No of moles} = \frac{2.59 \times 10^{-6}}{55880}$$

$$\text{Molar Concentration} = \frac{2.59 \times 10^{-6}}{55880 \times 10^{-6}}$$

Thus, Molar Concentration of purified L537 was calculated to be 46.34 μM .

4.2 Introduction of H173A mutation in L537 gene from Mimivirus

4.2.1 Cloning of L537 gene with H173A mutation in *E.coli* RIPL cells

4.2.1.1 DpnI Digestion of PCR product to remove template plasmid

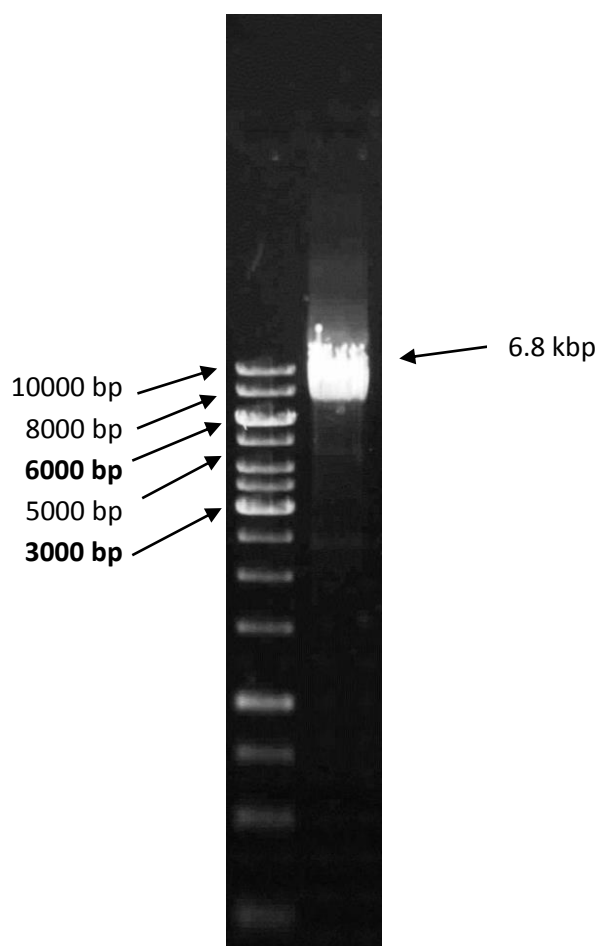


Figure 23. DpnI digested PCR product

Lane 1	DNA Ladder
Lane 2	PCR product

4.2.2 *E. coli* DH5 α competent cell preparation



Figure 24. *E. coli* competent cells successfully transformed with pET28a

4.2.3 *E. coli* DH5 α Plasmid Preparation

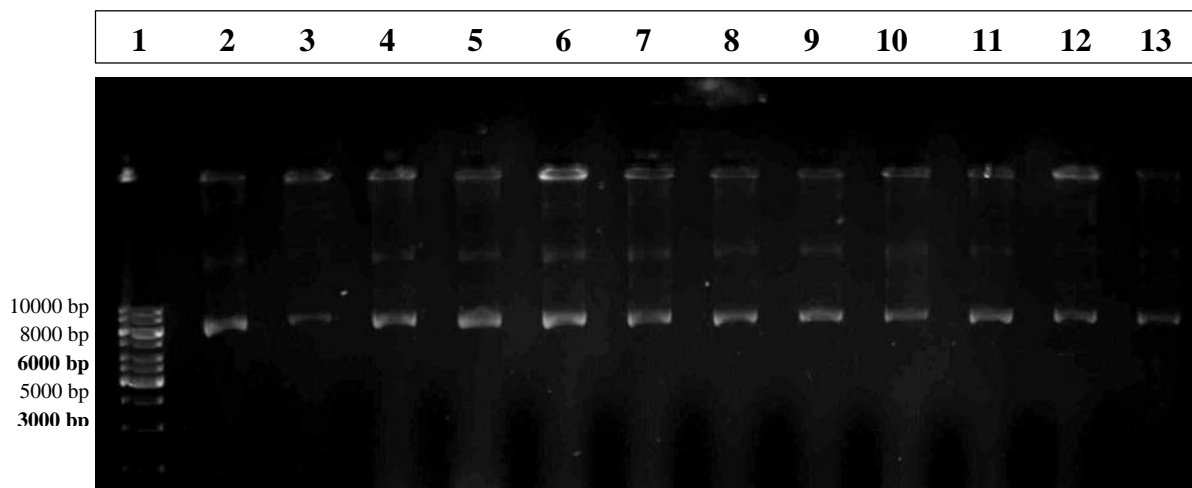


Figure 25. Plasmid purified from 12 clones of H173A DH5 α cells

Lane 1	DNA Ladder
Lane 2	Clone 1
Lane 3	Clone 2
Lane 4	Clone 3
Lane 5	Clone 4
Lane 6	Clone 5
Lane 7	Clone 6
Lane 8	Clone 7
Lane 9	Clone 8
Lane 10	Clone 9
Lane 11	Clone 10
Lane 12	Clone 11
Lane 13	Clone 12

4.2.4 H173A sequencing result (Clone 2)

L537 WT	1	MAEDKIEAYNKSITRTKYFKMDDAINSPICSKTVFIANERITKENRIGRYTVPFSFKK	60
H173A	1	MAEDKIEAYNKSITRTKYFKMDDAINSPICSKTVFIANERITKENRIGRYTVPFSFKK	60
L537 WT	61	FLKKRDSYPHCHEIIIDHINNKTNIAGRLVDFDIKITDSSILKDTGLIDKNDNQPIMFN	120
H173A	61	FLKKRDSYPHCHEIIIDHINNKTNIAGRLVDFDIKITDSSILKDTGLIDKNDNQPIMFN	120
L537 WT	121	SKTLSITKIPLNFKQQIENTIETIDQYFHDIDKTILEFIWSTSQNPNKFSK H LTVKNLY	180
H173A	121	SKTLSITKIPLNFKQQIENTIETIDQYFHDIDKTILEFIWSTSQNPNKFSK A LTVKNLY	180
L537 WT	181	FDDWITMSKLFYKLFCKVWDNQYYWISSKDLVDSQIVRNKGSLRMVGSTKINGYPLVFDN	240
H173A	181	FDDWITMSKLFYKLFCKVWDNQYYWISSKDLVDSQIVRNKGSLRMVGSTKINGYPLVFDN	240
L537 WT	241	KNHTLPDSLIRIYFRNHREKEQL	263
H173A	241	KNHTLPDSLIRIYFRNHREKEQL	263

Sequence alignment of the wild type L537 and mutant H173A shows the presence of a single mutation from Histidine to Alanine at position 173.

4.2.5 H173A induction at 30°C for 3 hours

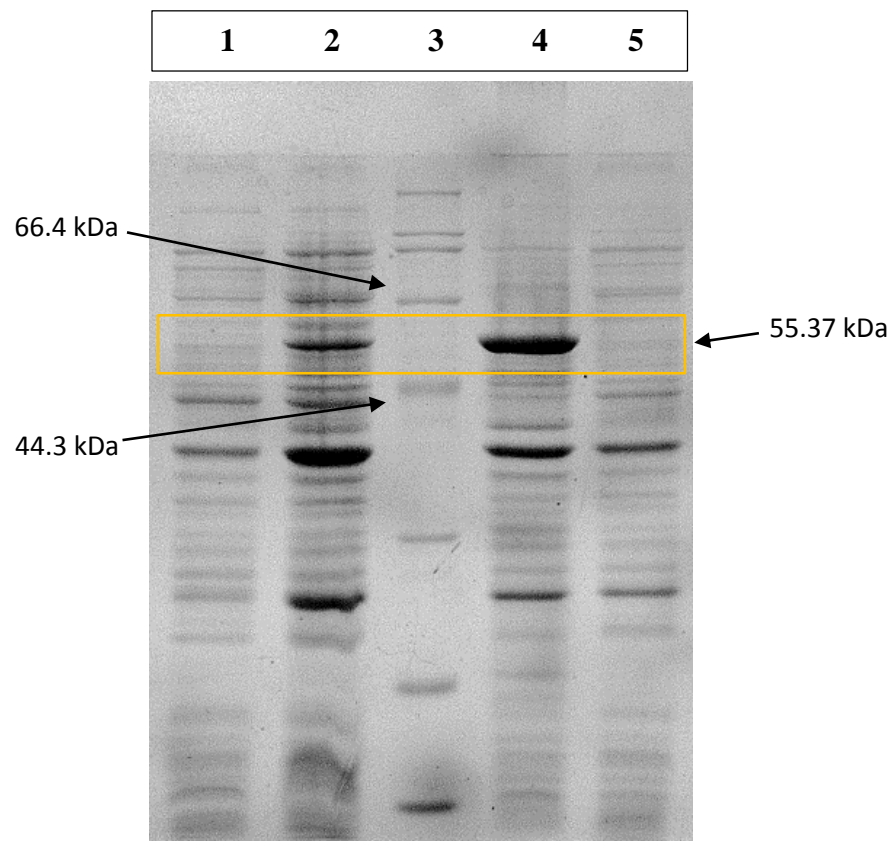


Figure 26. 3 hour induction at 30°C

Lane 1	-IPTG
Lane 2	+IPTG
Lane 3	Protein Ladder
Lane 4	Pellet after sonication
Lane 5	Supernatant after sonication

4.2.6 H173A induction at 25°C for 3 hours

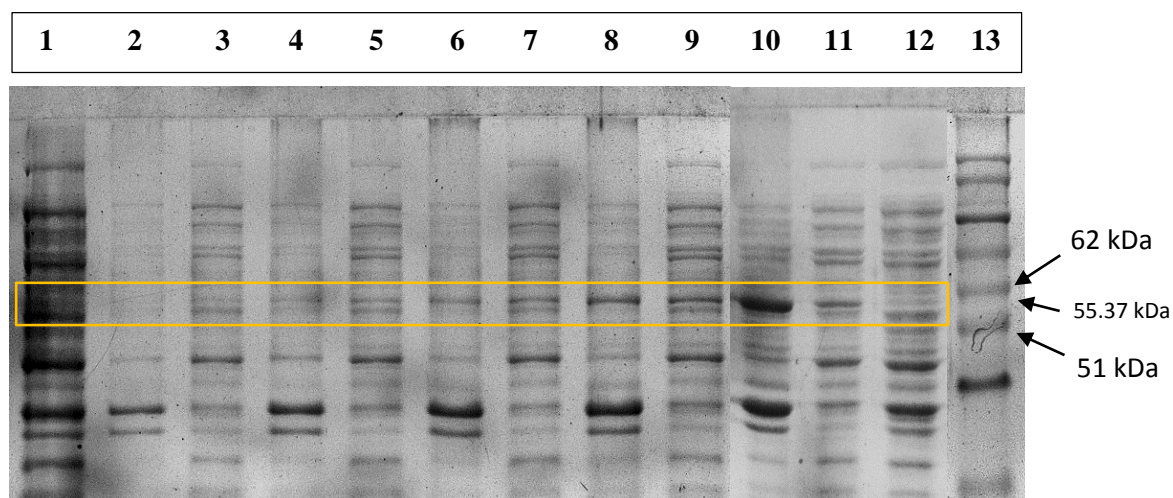


Figure 27. H173A induction gel

Lane 1	0 hour (-IPTG)
Lane 2	1 hour pellet (+IPTG)
Lane 3	1 hour supernatant (+IPTG)
Lane 4	1.5 hour pellet (+IPTG)
Lane 5	1.5 hour supernatant (+IPTG)
Lane 6	2 hour pellet (+IPTG)
Lane 7	2 hour supernatant (+IPTG)
Lane 8	2.5 hour pellet (+IPTG)
Lane 9	2.5 hour supernatant (+IPTG)
Lane 10	3 hour pellet (+IPTG)
Lane 11	3 hour supernatant (+IPTG)
Lane 12	3 hour (-IPTG)
Lane 13	Protein Ladder

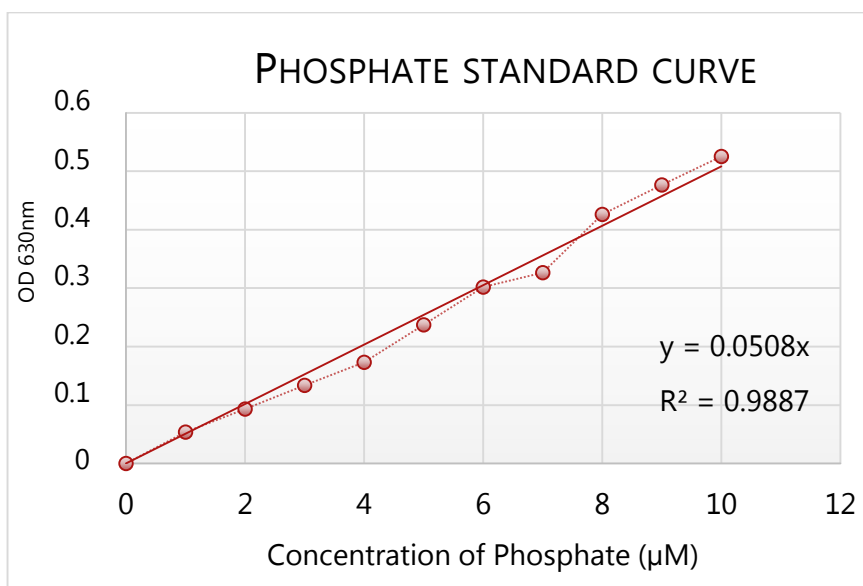
4.3 Estimation of Primase Activity

4.3.1 Malachite Green Assay

4.3.1.1 Phosphate Standard Curve

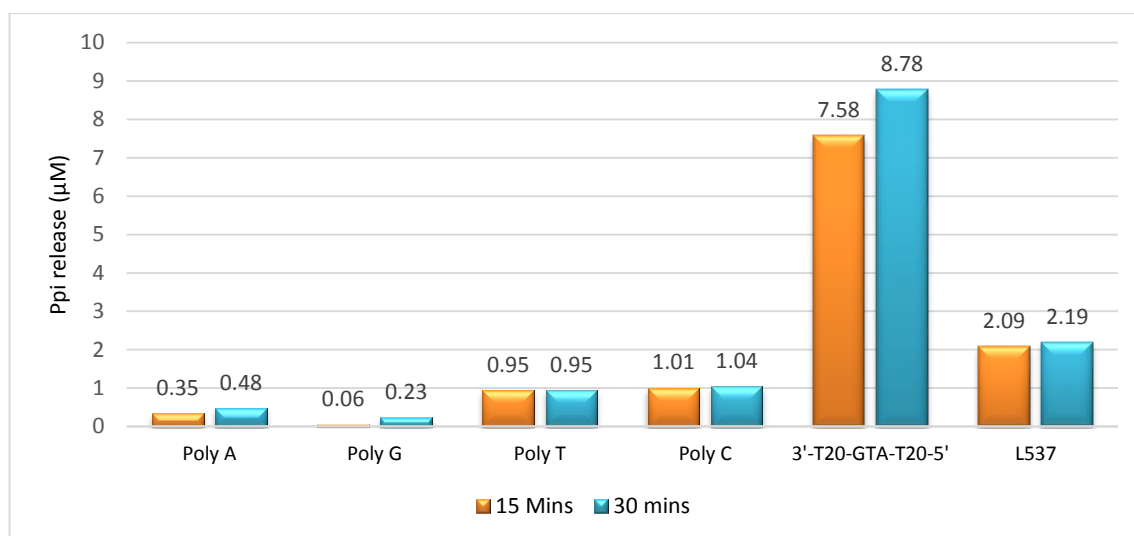
Table 16. Phosphate Standard curve

Conc. of Phosphate (μM)	OD 1	OD 2	OD ₆₃₀ avg
0	0	0	0
1	0.053	0.055	0.054
2	0.096	0.091	0.0935
3	0.135	0.133	0.134
4	0.174	0.172	0.173
5	0.24	0.235	0.2375
6	0.299	0.305	0.302
7	0.32	0.333	0.3265
8	0.408	0.445	0.4265
9	0.478	0.475	0.4765
10	0.515	0.536	0.5255



4.3.1.2 Assays for identification of the Priming site

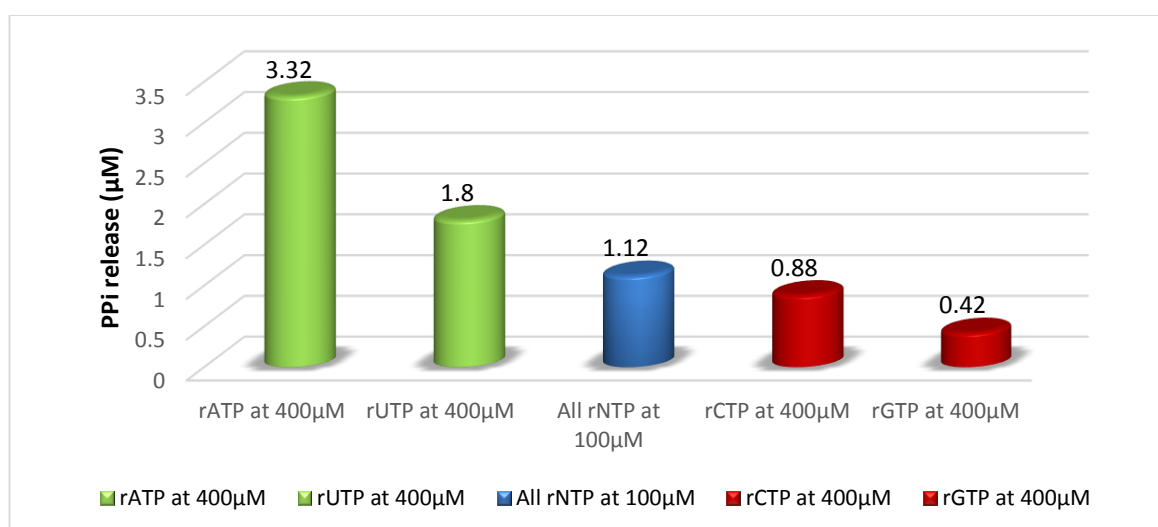
Primer synthesis with different templates



It was observed that the template 3' T20-GTA-T20 5' supports synthesis of longer primers as compared to homo oligomers and random templates.

Malachite green assay is a fast method of estimation of primase activity, but the length of primer synthesised cannot be estimated. Thus we cannot determine whether full length primers or truncated products are being formed.

Effect of different rNTP concentrations on primer synthesis



A recent study of HSV 1 primase by Ramirez & Kuchta, revealed many details about primase activity, it was observed that presence of higher concentrations of those rNTPs which are involved in the initial dimer synthesis promotes formation of longer primer products. We observed that, compared to the control, fourfold increase in rUTP and rATP resulted in higher primase activity.

CHAPTER 5

DISCUSSION AND CONCLUSIONS

Mimivirus belongs to the family Mimiviridae. It has many genes encoding proteins involved in replication, transcription and translation. It was found that replication in Mimivirus is not characterized at all and the role of the several replicative proteins is not known. From the previous sequence analysis carried out in the laboratory it was observed that the L537 gene from Mimivirus shows sequence similarity to archaeo eukaryotic primases. Thus, the first objective of this experiment was to purify the protein encoded by gene L537.

Previously, L537 gene had been cloned and expressed in *E. coli* RIPL DE3 cells. RIPL strains are engineered to contain extra copies of genes that encode the rare tRNAs which most frequently limit translation of heterologous proteins in *E. coli*. Thus, this strain was chosen to allow high level of expression of the viral protein.

Expression of the protein was induced by addition of 0.3 mM IPTG for 3 hours at 30°C. A band corresponding to ~55kDa was observed in samples induced for 3 hours when run along with sample collected before the addition of IPTG on a 12% SDS PAGE gel. On sonication of the cells it was observed that while most of the protein pellets down as insoluble inclusion bodies, a fraction of the protein remains soluble in the supernatant.

A polyhistidine-tag was added to L537 protein during its cloning, purification of the cell lysate was carried out by using Ni-NTA beads in a pre-packed column. An initial UV peak was observed for the unbound protein, on increasing the concentration of imidazole a single sharp peak was observed. A band was observed at ~55.37 kDa, along with some contaminating proteins when 0.5 ml fractions were collected at the peak and run on a 12% SDS PAGE gel.

Fractions containing the protein were pooled and concentrated to 2 ml and was injected to a Size Exclusion Chromatography column (superdex-200 column) for further purification. The peak corresponding to flow through was observed at 41.32 ml, followed by peak II and peak III at 64.73 ml and 70.69 ml respectively. Single sharp

bands corresponding to ~55.37 kDa were observed in the fractions collected at peak 2. L537 protein elutes in peak 2 which corresponds to ~ 65 ml. On comparison to the standard chart we see that the 65 ml corresponds to ~ 110 kDa. Thus, the protein probably exists as a dimer in its native state.

In order to carry out the activity assays, the concentration of isolated protein was estimated to be 45.6 μ M by Bradford assay and 38.8 μ M by determining the Optical Density at 280 nm. Because a variation was observed in the results, concentration was calculated by comparison with standard concentrations of BSA using ImageJ, It was calculated to be 46.3 μ M. Primase assays carried out using rNTPs confirm that L537 shows primase activity and it may be involved in the replication/repair mechanism in Mimivirus.

	MOTIF I	MOTIF II	MOTIF III	ZN FINGER MOTIF
L537 APMV	(90) FDFDI (74)	FSKHL (36)	LVDS (129)	KC(6)H(21)C(3)CS (91)
Acanthamoeba castellanii mamavirus	(90) FDIDV (48)	LSMHL (36)	LIDK (127)	KC(6)H(24)C(3)CN (10)
Acanthamoeba polyphaga lentillevirus	(90) FDFDI (74)	FSKHL (36)	LVDS (129)	KC(6)H(21)C(3)CS (6)
Megavirus chileensis	(86) FDFDI (48)	LSKHL (36)	LIDF (125)	NC(6)H(21)C(3)CY (41)
Moumouvirus goulette	(87) FDFDI (48)	LSKHL (36)	LIDF (124)	NC(6)H(21)C(3)CY (41)
Hirudovirus	(89) FDIDV (48)	LSMHL (36)	LIDK (127)	KC(3)H(24)C(3)CN (10)
L794 APMV	(90) FDIDV (48)	LSMHL (36)	LIDK (127)	KC(6)H(24)C(3)CN (10)
Ruminococcus sp.	(86) FDFDI (48)	LSKHL (36)	LIDF (125)	NC(6)H(21)C(3)CY (41)
Homo sapiens	(112) FDLEF (48)	FSRHL (107)	FVDL (136)	WC(6)H(19)C(4)CK (108)
Pan paniscus	(112) FDLEF (48)	FSRHL (25)	ALDL (218)	WC(6)H(19)C(4)CK (108)
Gorilla gorilla gorilla	(125) FDLEF (48)	FSRHL (25)	ALDL (218)	WC(6)H(19)C(4)CK (108)
Macaca fascicularis	(112) FDLEF (48)	FSRHL (25)	ALDL (214)	WC(6)H(19)C(4)CK (108)
Sulfolobus islandicus	(109) LDFES (27)	GGIHI (22)	IIDL (11)	SC(2)H(2)C(4)CP (707)
Acidianus ambivalens	(71) LDFED (27)	GGLHI (22)	VADL (11)	SC(2)H(2)C(4)CK (750)

Sequence alignment with known AEPs lead to the identification of conserved motifs in L537 protein- Dx D, sxH and h- and Zn finger motif (A. Gupta and K. Kondabagil, unpublished data). Thus, the second objective was to generate mutants to study the role of motif sxH hypothesized to be involved in DNA binding activity (Lipps et al. 2004).

Mutants were generated by site directed mutagenesis (Zheng et al. 2004). PCR was carried out using mutagenic primers, following which the PCR product is digested by DpnI. DpnI cleaves methylated sites thus acting only on the template plasmid but not on the PCR product. This step is important because the circular template plasmid has a transformation efficiency several orders of magnitude greater than the linear PCR product. The DpnI digested product shows the presence of a single band when run on a 0.8% Agarose gel.

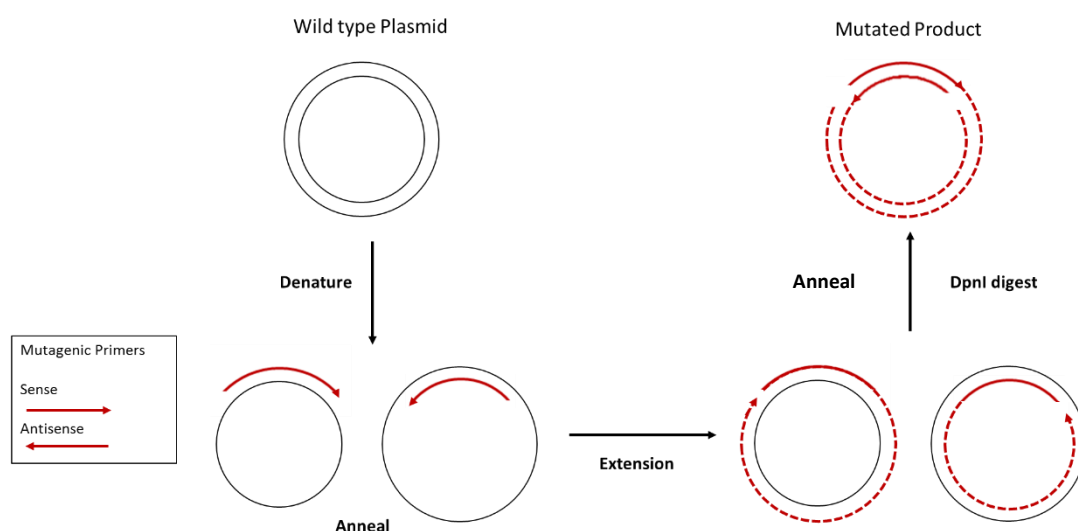


Figure 28. Mechanism of DpnI mediated mutagenesis

Competent cells were prepared, to verify their competency they were transformed with uncut pET28a and grown on Luria Agar plates with Kanamycin as a selection marker. Dh5 α competent cells were transformed with the mutant L537 H173A gene with the DpnI digested PCR product, and the cells were grown on Luria Agar plates with Kanamycin as a selection marker. The transformants were picked after overnight incubation at 37 °C and plasmid isolation was carried out from 12 clones.

Isolated plasmids were transformed into RIPL competent cells and grown on Luria Agar plates with Kanamycin and Chloramphenicol as a selection marker. After overnight incubation at 37 °C transformant colonies were checked for protein expression by IPTG induction. Clones which expressed the protein were sequenced to verify the presence of mutation. Sequencing results confirm Histidine to Alanine mutation in L537 at position 173 in clone 2.

Expression in RIPL cells with H173A mutation was induced by IPTG at 30 °C for 3 hours. But it was observed that all of the protein forms insoluble inclusion bodies, and thus the protein was not present in the soluble form. It was hypothesized that due to the mutation there was a reduced protein stability and the induction temperature was reduced to 25 °C, samples were collected after half hour durations and run on an SDS PAGE gel. It was seen that on induction at 25 °C, for 2.5 hours about half of the protein exists in the soluble form. So further purification can be carried out with this optimized procedure.

The next objective was to characterize this primase encoded by gene L537. Efforts were focussed on identifying the tri-nucleotide priming site of the primase. Previous studies carried out in the laboratory revealed that as compared to rATP, rCTP and rUTP omission of rGTP does not affect primer synthesis significantly using random templates. Hence, it was hypothesized that the priming site on the template may not contain deoxyribonucleotide C and it could be a combination of A, T and G deoxyribonucleotides, also among homo oligomers poly(T) showed good activity. . Different templates were synthesised containing various combination of A, T and G flanked by deoxythymidates.

Table 17. Templates used for priming site identification

T ₂₀ -GTA-T ₂₀	T ₂₀ -TGA-T ₂₀	T ₂₀ -AGT-T ₂₀
T ₂₀ -GAT-T ₂₀	T ₂₀ -TAG-T ₂₀	T ₂₀ -ATG-T ₂₀

Comparison of primer synthesis with the different synthetic templates was carried out and it was observed that 3' T₂₀-GTA-T₂₀ 5' supported synthesis of longer primers as compared to poly(A), poly(G), poly(T), poly(C) and templates with random sequences. Thus, the template 3' T₂₀-GTA-T₂₀ 5' could contain the priming site. Ramirez and Kuchta reported that the initial dinucleotide formation is the rate determining step. Thus, to test this hypothesis we designed an experimental setup in which only the substrates required for the dinucleotide formation were increased, to check its effect on total primer synthesis. rATP, rUTP, rCTP and rGTP were increased four-fold as compared to the rest of the rNTPs, a control was taken in which all rNTPs were kept constant at 100 μ M. With the template tested (T₂₀GTAT₂₀) it was observed that increasing the concentration of rATP and rUTP from 100 μ M to 400 μ M both ribonucleotides involved in the initial dimer formation increased total primer synthesis, whereas increasing the concentration of ribonucleotides rCTP and rGTP both of which are not involved in dinucleotide formation rather inhibited primer synthesis. Similar primase activity was also reported with HSV-1 primase helicase (Ramirez-Aguilar & Kuchta 2004). However, the increase in total primer synthesis with rATP can also accounted to be due to the T₂₀ flanking sequences.

Further tests are required to confirm this. Assays with radiolabelled α -³²P and γ -³²P rNTPs can be performed to observe lengths of the primer which are synthesized.

CHAPTER 6

FUTURE WORK

1. Purification of L537 protein with H173A mutation from *E. coli* RIPL cells.
2. Primer synthesis studies using α -³²P and γ -³²P rNTPs, to determine the size primers being synthesised by wild-type and mutant L537.
3. Comparative study of the primer synthesis kinetics of the wild-type and mutant L537 on ssDNA templates.

CHAPTER 7

BIBLIOGRAPHY

- Abergel, C. et al., 2005. Mimivirus TyrRS: Preliminary structural and functional characterization of the first amino-acyl tRNA synthetase found in a virus. *Acta Crystallographica Section F: Structural Biology and Crystallization Communications*, 61(2), pp.212–215.
- Abrahão, J.S. et al., 2014. Acanthamoeba polyphaga mimivirus and other giant viruses: an open field to outstanding discoveries. *Virology journal*, 11(1), p.120. Available at: <http://www.virologyj.com/content/11/1/120>.
- Aravind, L., Leipe, D.D. & Koonin, E. V., 1998. Toprim - A conserved catalytic domain in type IA and II topoisomerases, DnaG-type primases, OLD family nucleases and RecR proteins. *Nucleic Acids Research*, 26(18), pp.4205–4213.
- Benarroch, D. & Shuman, S., 2006. Characterization of mimivirus NAD⁺-dependent DNA ligase. *Virology*, 353(1), pp.133–143.
- Biswas, T. et al., 2013. A novel non-radioactive primase-pyrophosphatase activity assay and its application to the discovery of inhibitors of Mycobacterium tuberculosis primase DnaG. *Nucleic Acids Research*, 41(4), pp.1–13.
- Boudet, J. et al., 2015. Structures to complement the archaeo-eukaryotic primases catalytic cycle description: What's next? *Computational and Structural Biotechnology Journal*, pp.1–13. Available at: <http://linkinghub.elsevier.com/retrieve/pii/S2001037015000252>.
- Campos, R.K. et al., 2014. Samba virus: a novel mimivirus from a giant rain forest, the Brazilian Amazon. *Virology Journal*, 11(1), p.95. Available at: <http://www.virologyj.com/content/11/1/95>.
- Claverie, J.M. et al., 2009. Mimivirus and Mimiviridae: Giant viruses with an increasing number of potential hosts, including corals and sponges. *Journal of Invertebrate Pathology*, 101(3), pp.172–180. Available at: <http://dx.doi.org/10.1016/j.jip.2009.03.011>.
- Claverie, J.-M. & Abergel, C., 2009. Mimivirus and its virophage. *Annual review of genetics*, 43, pp.49–66.
- Colson, P. et al., 2012. Reclassification of giant viruses composing a fourth domain of life in the new order Megavirales. *Intervirology*, 55(5), pp.321–332.
- Colson, P. et al., 2011. The giant Cafeteria roenbergensis virus that infects a widespread marine phagocytic protist is a new member of the fourth domain of life. *PLoS ONE*, 6(4), pp.13–17.

- Copeland, W.C. & Wang, T.S.F., 1993. Enzymatic characterization of the individual mammalian primase subunits reveals a biphasic mechanism for initiation of DNA replication. *Journal of Biological Chemistry*, 268(35), pp.26179–26189.
- Crute, J.J. et al., 1989. Herpes simplex virus 1 helicase-primase: a complex of three herpes-encoded gene products. *Proceedings of the National Academy of Sciences of the United States of America*, 86(7), pp.2186–2189.
- Desogus, G. et al., 1999. Identification and characterization of a DNA primase from the hyperthermophilic archaeon *Methanococcus jannaschii*. *Nucleic acids research*, 27(22), pp.4444–4450.
- Filée, J., 2013. Route of NCLDV evolution: The genomic accordion. *Current Opinion in Virology*, 3(5), pp.595–599.
- Filée, J. & Chandler, M., 2010. Gene exchange and the origin of giant viruses. *Intervirology*, 53(5), pp.354–361.
- Forterre, P., 2011. A new fusion hypothesis for the origin of Eukarya: Better than previous ones, but probably also wrong. *Research in Microbiology*, 162(1), pp.77–91. Available at: <http://dx.doi.org/10.1016/j.resmic.2010.10.005>.
- Forterre, P., 2010. Defining Life: The Virus Viewpoint. *Origins of Life and Evolution of Biospheres*, 40(2), pp.151–160.
- Forterre, P., Krupovic, M. & Prangishvili, D., 2014. Cellular domains and viral lineages. *Trends in Microbiology*, 22(10), pp.554–558. Available at: <http://dx.doi.org/10.1016/j.tim.2014.07.004>.
- García-Gómez S, Reyes A, Martínez-Jiménez MI, Chocrón ES, Mourón S, Terrados G, Powell C, Salido E, Méndez J, Holt IJ, B.L., 2013. Article PrimPol , an Archaic Primase / Polymerase Operating in Human Cells. *Molecular biology of the cell*, pp.1–13.
- Gill, S. et al., 2014. A highly divergent archaeo-eukaryotic primase from the *Thermococcus nautilus* plasmid, pTN2. *Nucleic Acids Research*, 42(6), pp.3707–3719.
- Ichardson, C.H.C.R., 1999. The Cys 4 zinc finger of bacteriophage T7 primase in sequence-specific single-stranded DNA recognition. , 96(April), pp.4295–4300.
- Iyer, L.M. et al., 2006. Evolutionary genomics of nucleo-cytoplasmic large DNA viruses. *Virus Research*, 117(1), pp.156–184.
- Iyer, L.M. et al., 2005. Origin and evolution of the archaeo-eukaryotic primase superfamily and related palm-domain proteins: Structural insights and new members. *Nucleic Acids Research*, 33(12), pp.3875–3896.

- Iyer, L.M., Aravind, L. & Koonin, E. V, 2001. Common Origin of Four Diverse Families of Large Eukaryotic DNA Viruses Common Origin of Four Diverse Families of Large Eukaryotic DNA Viruses. , 75(23), pp.11720–11734.
- Jeudy, S. et al., 2012. Translation in Giant Viruses: A Unique Mixture of Bacterial and Eukaryotic Termination Schemes. *PLoS Genetics*, 8(12).
- Koonin, E. V, 2005. Virology: Gulliver among the Lilliputians. *Current biology : CB*, 15(5), pp.R167–9. Available at: <http://www.sciencedirect.com/science/article/pii/S0960982205002137> [Accessed May 25, 2015].
- Lee, J.-B. et al., 2006. DNA primase acts as a molecular brake in DNA replication. *Nature*, 439(7076), pp.621–624.
- Lee, S.J. et al., 2012. Zinc-binding domain of the bacteriophage T7 DNA primase modulates binding to the DNA template. *Journal of Biological Chemistry*, 287(46), pp.39030–39040.
- Legendre, M. et al., 2014. Thirty-thousand-year-old distant relative of giant icosahedral DNA viruses with a pandoravirus morphology. *Proceedings of the National Academy of Sciences of the United States of America*, 111(11), pp.4274–9. Available at: <http://www.ncbi.nlm.nih.gov/pubmed/24591590>.
- Lipps, G. et al., 2004. Structure of a bifunctional DNA primase-polymerase. *Nature structural & molecular biology*, 11(2), pp.157–162.
- Mutsa, Y. et al., 2014. Infection cycles of large DNA viruses : Emerging themes and underlying questions. , 467, pp.3–14.
- Mutsafi, Y. et al., 2013. Membrane Assembly during the Infection Cycle of the Giant Mimivirus. *PLoS Pathogens*, 9(5).
- Mutsafi, Y. et al., 2010. Vaccinia-like cytoplasmic replication of the giant Mimivirus. *Proceedings of the National Academy of Sciences of the United States of America*, 107(13), pp.5978–5982.
- Ramirez-Aguilar, K. a. & Kuchta, R.D., 2004. Mechanism of Primer Synthesis by the Herpes Simplex Virus 1 Helicase-Primase. *Biochemistry*, 43(6), pp.1754–1762.
- Ramirez-Aguilar, K. a., Low-Nam, N. a. & Kuchta, R.D., 2002. Key role of template sequence for primer synthesis by the herpes simplex virus 1 helicase-primase. *Biochemistry*, 41(49), pp.14569–14579.
- Raoult, D. et al., 2004. The 1 . 2-Megabase Genome Sequence of Mimivirus. *Science*, 306(5700), pp.1344–1350. Available at: <http://www.ncbi.nlm.nih.gov/pubmed/15486256>.

- Raoult, D. & Forterre, P., 2008. Redefining viruses: lessons from Mimivirus. *Nature reviews. Microbiology*, 6(4), pp.315–319.
- Raoult, D., La Scola, B. & Birtles, R., 2007. The discovery and characterization of Mimivirus, the largest known virus and putative pneumonia agent. *Clinical infectious diseases : an official publication of the Infectious Diseases Society of America*, 45(1), pp.95–102.
- La Scola, B. et al., 2003. A giant virus in amoebae. *Science (New York, N.Y.)*, 299(5615), p.2033.
- La Scola, B. et al., 2005. Mimivirus in pneumonia patients. *Emerging Infectious Diseases*, 11(3), pp.449–452.
- Suzan-Monti, M., La Scola, B. & Raoult, D., 2006. Genomic and evolutionary aspects of Mimivirus. *Virus Research*, 117(1), pp.145–155.
- Yamada, T., 2011. Giant viruses in the environment: Their origins and evolution. *Current Opinion in Virology*, 1(1), pp.58–62. Available at: <http://dx.doi.org/10.1016/j.coviro.2011.05.008>.
- Yutin, N. & Koonin, E. V, 2012. Hidden evolutionary complexity of Nucleo-Cytoplasmic Large DNA viruses of eukaryotes. *Virology Journal*, 9(1), p.161.
- Yutin, N., Wolf, Y.I. & Koonin, E. V, 2014. Origin of giant viruses from smaller DNA viruses not from a fourth domain of cellular life. , 467, pp.38–52.
- Zauberman, N. et al., 2008. Distinct DNA exit and packaging portals in the virus *Acanthamoeba polyphaga* mimivirus. *PLoS Biology*, 6(5), pp.1104–1114.
- Zheng, L., Baumann, U. & Reymond, J., 2004. An efficient one-step site-directed and site-saturation mutagenesis protocol. , 32(14).

CHAPTER 8

APPENDICES

Table 18. Preparation of SDS PAGE gel

Reagent	Resolving Gel (12%, 10ml)	Stacking Gel (2ml)
H ₂ O	3.3ml	1.4ml
Acrylamide	4ml	330µl
1.5M Tris (pH 8.8)	2.5ml	-
1M Tris (pH 6.8)	-	250µl
10% SDS	100µl	20µl
APS	100µl	20µl
TEMED	4µl	2µl

Table 19. Preparation of 4X Loading Dye

Reagent	Amount
1M Tris HCl (pH 6.8)	0.6ml
Glycerol	2.5ml
Bromophenol	0.004g
Water	3.9ml
10% SDS	3ml

5 µl of betamercaptoethanol was added to 95 µl of above solution to make working solution of 100 µl.

Samples for SDS PAGE were prepared by adding 5ul of 4X Loading Dye to 15ul of sample.

Sonication was performed at 40% Amplitude with 2 second pulses.

Table 20. Preparation of 1 Litre staining solution

Reagent	Amount
Coomassie 250	2.5g
Glacial acetic acid	100ml
Methanol	400ml
Distilled water	500ml

Table 21. Preparation of 1 Litre destaining solution

Reagent	Amount
Glacial acetic acid	100ml
Methanol	200ml
Distilled water	700ml

Calibration of Superdex-200 pg size exclusion chromatography column

Calibration was carried out by using standard markers such as Amylase, ADH, BSA, Carbonic anhydrase and Cytochrome C (Table 3). Blue dextran was used for calibration of void volume (V_0).

Table 22. Elution volume (V_e), log(MW) and K_{av} for standard markers.

Sr no.	Standards	Mol. Wt (Da)	Log (MW)	V_e	K_{av}
1	B-Amylase	200000	5.30	59.51	0.19
2	ADH	150000	5.18	64.06	0.25
3	BSA	66000	4.82	70.92	0.34
4	Carbonic anhydrase	29000	4.46	85.29	0.53
5	Cytochrome C	12400	4.09	95	0.66
6	Blue dextran	2000000	6.30	45.02	Void volume

K_{av} for preparation of calibration curve was calculated using following formula:

$$K_{av} = \frac{V_e - V_0}{V_t - V_0}$$

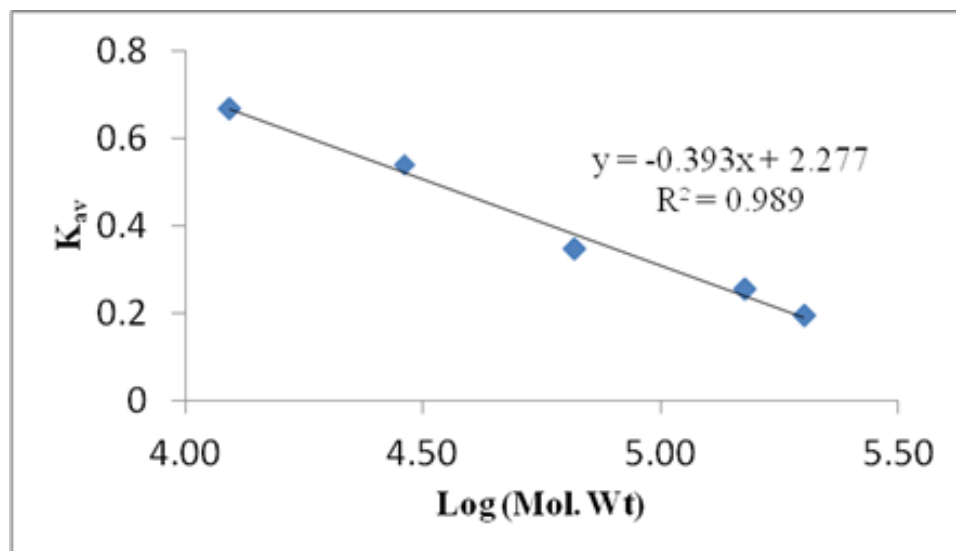


Figure 29. Calibration curve (Superdex 200 pg)

Table 23. Composition of Affinity Chromatography buffers

Binding Buffer	Elution Buffer
0.5M NaCl	0.5M NaCl
50mM Tris HCl	50mM Tris HCl
5mM MgCl ₂	5mM MgCl ₂
10mM Imidazole	600mM Imidazole
10% glycerol	10% glycerol

Table 24. Composition of Gel filtration chromatography buffers

Equilibration buffer
0.5M NaCl
50mM Tris HCl
1% glycerol

Table 25. Plasmid purification buffers (Miniprep)

Buffer	Composition
Alkaline Lysis Buffer I	TE + RNAase
Alkaline Lysis Buffer II	0.2N NaOH + 10% SDS
Alkaline Lysis Buffer III	Potassium Acetate (pH 5.2)